

AD A 0 4 7 9 7 5

12

AV-E 300 062

DNA 4019T

# PROPAGATION IN STRIATED MEDIA

Mission Research Corporation  
735 State Street  
Santa Barbara, California 93101

May 1976

Topical Report for Period April 1976—May 1976

CONTRACT No. DNA 031-76-C-0135

APPROVED FOR PUBLIC RELEASE;  
DISTRIBUTION UNLIMITED.

THIS WORK SPONSORED BY THE DEFENSE NUCLEAR AGENCY  
UNDER RDT&E RMSS CODE B322076484 S99QAXHB04505 H2590D.

AD No. \_\_\_\_\_  
DDC FILE COPY

Prepared for  
Director  
DEFENSE NUCLEAR AGENCY  
Washington, D. C. 20305

DDC  
RECEIVED  
DEC 28 1977  
B

## **DISCLAIMER NOTICE**

**THIS DOCUMENT IS BEST QUALITY PRACTICABLE. THE COPY FURNISHED TO DTIC CONTAINED A SIGNIFICANT NUMBER OF PAGES WHICH DO NOT REPRODUCE LEGIBLY.**

Destroy this report when it is no longer  
needed. Do not return to sender.



18 DNI, SBIE

UNCLASSIFIED

SECURITY CLASSIFICATION OF THIS PAGE (When Data Entered)

REPORT DOCUMENTATION PAGE		READ INSTRUCTIONS BEFORE COMPLETING FORM
1. REPORT NUMBER DNA 4019T, HD-E300 042	2. GOVT ACCESSION NO.	3. RECIPIENT'S CATALOG NUMBER
4. TITLE (and Subtitle) PROPAGATION IN STRIATED MEDIA	5. TYPE OF REPORT Topical Report for Period Apr 28 - May 76	6. PERFORMING ORG. REPORT NUMBER MRC-R-118
7. AUTHOR(S) R. W. Hendrick L. Shaeffer	8. CONTRACT OR GRANT NUMBER(S) DNA 001-76-C-0135 / None	9. PROGRAM ELEMENT, PROJECT, TASK AREA & WORK UNIT NUMBERS NWED Subtask, S99QAXH0454-05
10. PERFORMING ORGANIZATION NAME AND ADDRESS Mission Research Corporation 735 State Street Santa Barbara, California 93101	11. CONTROLLING OFFICE NAME AND ADDRESS Director Defense Nuclear Agency Washington, D.C. 20305	12. REPORT DATE May 1976
13. MONITORING AGENCY NAME & ADDRESS (if different from Controlling Office) 82p.	14. NUMBER OF PAGES 86	15. SECURITY CLASS. (of this report) UNCLASSIFIED
16. DISTRIBUTION STATEMENT (of this Report) Approved for public release; distribution unlimited.		
17. DISTRIBUTION STATEMENT (of the abstract entered in Block 20, if different from Report)		
18. SUPPLEMENTARY NOTES This work sponsored by the Defense Nuclear Agency under RDT&E RMSS Code B322076464 S99QAXH04505 H2590D.		
19. KEY WORDS (Continue on reverse side if necessary and identify by block number) Radar Propagation Scattering Inhomogeneous Media		
20. ABSTRACT (Continue on reverse side if necessary and identify by block number) The propagation of radar through a striated plasma has been analyzed on the basis of random walk photon scattering, geometric optics refraction at a thin phase screen, plane wave scattering from a thin screen in the Fraunhofer limit and the observables to a monopulse system using a wave front integration implementation of Huygens' principle over a thin phase screen. The latter two were carried out for screens of both large and small phase variance. The scattering was related to the properties of the plasma for a variety of distribution functions of striation sizes. For reasonable distributions, a similar		

DD FORM 1473 EDITION OF 1 NOV 65 IS OBSOLETE

UNCLASSIFIED

SECURITY CLASSIFICATION OF THIS PAGE (When Data Entered)

406 548

HB

UNCLASSIFIED

SECURITY CLASSIFICATION OF THIS PAGE (When Data Entered)

20. ABSTRACT (Continued)

effective striation size is obtained. This allows the calculation of the angular variance of the scattered power which is gaussianly distributed for most significant cases. In the geometric optics regime the distribution of density of allowable multipath rays is gaussianly distributed and the power distribution is identical for all rays. The signal processor sees an unmodified but attenuated component and a random-phased, scattered component that leads to Rician amplitude statistics. The results of the various approaches are all compatible and furnish a single unified description of the perturbed signal. ←

ACCESSION for		
NTIS	White Section	<input checked="" type="checkbox"/>
DDC	Buff Section	<input type="checkbox"/>
UNANNOUNCED		<input type="checkbox"/>
JUSTIFICATION		
BY		
DISTRIBUTION/AVAILABILITY CODES		
Dist. AVAIL. and/or SPECIAL		
A		

UNCLASSIFIED

SECURITY CLASSIFICATION OF THIS PAGE (When Data Entered)

## PREFACE

The work described here was originally performed in early 1974 for the U.S. Army SAFEGUARD System Command, and was directed toward the description of the behavior of a UHF radar operating in a strongly scattering medium. Any large-scale structure (tens of kilometers) was handled by gross refraction computations and only the fine-scale structure was assumed to be handled by the scattering analysis. Most aspects of the analysis covered here are precisely applicable only in the limit that plasma structural dimensions are small compared to a Fresnel zone. This assumption is identical to the assumption that the receiving antenna is in the far zone of the scattering medium when it is considered to be a transmitting source. Recent research has shown that extreme care is necessary in the extension of theory to higher frequencies where the structural assumptions may not be valid.

## CONTENTS

<u>Section</u>	<u>Page</u>
PREFACE	1
LIST OF FIGURES	4
1. PROBLEM STATEMENT	5
2. THEORETICAL AND EXPERIMENTAL BACKGROUND	6
2.1 Plasma Induced Phase Shift	6
2.2 Striation Profile	7
2.3 Experimental Striation Size Distribution	8
2.4 Striations Outside Fireballs	9
3. PROPAGATION ANALYSIS	10
3.1 Random Walk Approach to Scattering	10
3.2 Phase Screen Approximation to Strong Scattering	13
3.3 Ray Optics and Stationary Phase Analysis	21
3.3.1 Scattering as Viewed by the Radar	21
3.3.2 Distribution in Phase, Angle and Power	23
3.3.3 Density of Multipath Returns	27
3.4 Huygens' Wave Theory and Angular Power Spectrum	28
3.4.1 Autocorrelation Function of Electric Field	29
3.4.2 Unmodified Components	30
3.4.3 Unmodified Signal	31
3.4.4 Large Phase Perturbation Scattered Signal	33
3.4.5 Small Phase Variance Scattered Signal	34
3.4.6 Variance of Angle of Arrival for Uniform Striations	36
3.4.7 Summary	38
3.5 Monopulse Response to Scattering	39
3.5.1 Sum and Difference Channel Signal Formulations	40
3.5.2 Sum Channel Power	43

CONTENTS (Continued)

<u>Section</u>	<u>Page</u>
3.5.3 Sum Channel Amplitude Distribution	50
3.5.4 Difference Channel Power	53
3.5.5 Summary of Monopulse System Output	56
4. SCATTERING BY VARIOUS PLASMA STRUCTURES	58
4.1 Model Descriptions	58
4.1.1 Model 1	59
4.1.2 Model 2	59
4.1.3 Model 3	62
4.1.4 Model 4	62
4.2 Plasma Parameters	63
4.2.1 Model 1	64
4.2.2 Model 2	65
4.2.3 Model 3	67
4.2.4 Model 4	67
5. SUMMARY AND UTILIZATION OF FORMULATIONS	69
5.1 Local Effective Striation Size	69
5.2 Local Scattering Angle	69
5.3 Local Phase Variance	70
5.4 Integrated Scattering Angle	70
5.5 Integrated Phase Variance and Mean Striation Size	71
5.6 Angular Scattering of Power	71
5.7 Received Power Statistics	72
5.8 Difference Channel Signal	73
5.9 Limitations	74
REFERENCES	75
APPENDIX A. A USEFUL INTEGRAL	77

## LIST OF FIGURES

<u>Figure</u>		<u>Page</u>
1	Scatter geometry	21
2	Antenna-scattering configuration	40
3	Probability density function for Model 2	60
4	Effective striation sizes for the various scattering models	66

## 1. PROBLEM STATEMENT

The detonation of nuclear weapons above about 80 km results in extensive regions of ionization—partially ionized plasmas. Detonation induced winds may blow this plasma across the geomagnetic field in a way that results in instabilities in the ionized component. Such instabilities produce striations extended along the geomagnetic field lines. These striations have been seen on all nuclear tests at very high altitudes.

If radars attempt measurements through striated regions, the wave fronts are broken up, resulting in scattering and multipath propagation. The quantification of the effects produced by striations has continued in the effort reported here. Specifically, additional analysis has unified prior work, extended models of the effects to weak scattering cases, removed some arbitrary assumptions, identified limits of applicability of previous models and considered the sensitivity to various assumptions about plasma structure. Current theoretical plasma analysis yields little information about striation ionization profiles or distribution of striation sizes. Consequently, unless a relative insensitivity to these plasma parameters is demonstrated, modeling of the derived effects will have limited utility.

Several approaches to the scattering problem will be considered. Each has its own region of validity and limitations and is useful to illustrate particular aspects of the scattering. Specifically, the first approach will be a photon scattering analysis that is valid for conditions under which photons are phase-incoherent. Subsequent approaches will use the approximation that the inhomogeneous medium is relatively localized and can be approximated by combining the integrated plasma induced phase shift in a single, thin, phase shifting screen. General characteristics, valid when geometric

optics approximations apply, will be derived. A physical optics analysis using Huygens' principle will obtain a generalized angular power spectrum for cases of either small or large phase perturbations. Following these basic scattering analyses, the interpretation of the multipath signal by a phase comparison monopulse system will be developed, the sensitivity to alternate models explored and scattering in terms of plasma parameters summarized.

## 2. THEORETICAL AND EXPERIMENTAL BACKGROUND

### 2.1 Plasma Induced Phase Shift

For radar waves (which have frequencies much greater than either electron collision or gyro-frequencies), the index of refraction of a plasma is given by

$$\mu^2 = 1 - \frac{n_e e^2}{m \epsilon_0 \omega^2}, \quad (1)$$

where  $\epsilon_0$  is the permittivity of free space,  $n_e$  is the electron concentration,  $e$  and  $m$  are the electronic charge and mass and  $\omega$  is the radar angular frequency. Denote a critical electron content

$$n_c = \omega^2 m \epsilon_0 / e^2, \quad (2)$$

so that

$$\mu^2 = 1 - n_e / n_c. \quad (3)$$

For conditions of interest to radar propagation, usually  $n_e \ll n_c$ . Consequently,

$$\mu \approx 1 - n_e/2n_c \quad (4)$$

This approximation will be used in the remainder of this report.

The electric vector of a plane wave propagating in a plasma is given by

$$E(x, t) = E_0 e^{i\left(\omega t - \frac{\omega x \mu}{c}\right)} \quad (5)$$

This means the phase is

$$\phi(x, t) = \omega t - \omega x \mu / c \quad (6)$$

Compared to a wave in the absence of plasma ( $\mu = 1$ ), the phase advance per unit path is

$$\frac{d\phi}{dx} = \frac{\omega(1 - \mu)}{c} = \frac{\omega}{c} \frac{n_e}{2n_c} \quad (7)$$

## 2.2 Striation Profile

For most of the detailed analysis in this report, the individual striations will be assumed to be cylindrically symmetric and have an electron concentration profile that is gaussian. There is no experimental data to support or contradict this assumption. If the profile were controlled exclusively by diffusion and the diffusion coefficient were constant, it would be gaussian. However, the real rationale for using this model is that it renders the mathematics tractable. The justification for acceptance of the results is that where alternate assumptions can be used, the results are not significantly altered. Some of these cases will be pointed out in the following discussions.

The electron concentration will be given by

$$n_e = n_0 e^{-\frac{r^2}{2\sigma^2}}, \quad (8)$$

where  $n_0$  is the axial electron concentration,  $r$  is the distance from the axis and  $\sigma$  is the characteristic dimension of the striation. Distributions of sizes will be considered and  $n_0$  may be a function of  $\sigma$ .

### 2.3 Experimental Striation Size Distribution

The only experimental data on striation size distributions for nuclear events comes from photographic data. Thus, it is limited to regions of optical emission, the highly disturbed or fireball regions. There is theoretical basis for believing that striations also form outside high altitude fireballs. It must be remembered then that the experimental data is obtained from only one type of unstable region and is not necessarily representative of all such regions.

Pertinent photographic data have been analyzed by W. Chesnut<sup>(1)</sup>, SRI, and the data can be reasonably well fit by gaussian striations with constant on-axis concentration and a size distribution

$$P(\sigma) = \frac{8}{3\sqrt{\pi}} \frac{\sigma_0^6}{\sigma_0} e^{-\left(\frac{\sigma_0}{\sigma}\right)^2} \quad (9)$$

Some of the data were best fit by the superposition of two distributions, each of the form of Equation 9. Also, the quality of the data is insufficient to define the exponent of the  $\sigma_0/\sigma$  term very well—5 or 7 might be as good as 6. But, use of the sixth power makes some desired integrals closed, well known analytic functions.

## 2.4 Striations Outside Fireballs

Theoretical analysis<sup>(2)</sup> has shown that where the direction of the explosion induced wind is both generally crossing the geomagnetic field lines and in the direction of decreasing electron content, the ionized fluid flow is unstable and should develop perturbations (and possibly striations). Spatial structure of characteristic wavelength greater than a minimum cutoff wavelength  $\lambda_c$  should grow.

If the environment is assumed to be composed of the superposition of a large number of such Fourier components, the spatial amplitude of which is limited to the spatial wavelength, the number of striations tends to fall off as an inverse power of the striation size. Below a minimum size, the population should be nearly zero. The amplitude of the disturbance may be a function of the striation size. Previous HARC<sup>(3)</sup> analysis assumed that the concentration perturbation  $n_0$  was proportional to the striation wavelength (due to interchanging air over a region a wavelength long) and that the appropriate power law was the inverse fourth.\*

It is necessary to relate cutoff wavelength and minimum striation size. In the HARC work, the sine wave, Fourier components were approximated

---

\* The number of striations of a given size per unit area perpendicular to the magnetic field was taken to be inversely proportional to the size and proportional to the allowed mode density on a circular ring. The mode density is then

$$n = \frac{2\pi R}{\lambda}$$

$$\frac{dn}{d\lambda} = \frac{2\pi R}{\lambda^2}$$

Thus,

$$P(\lambda) = \frac{a}{\lambda^2} \frac{dn}{d\lambda} = \frac{a^2 R}{\lambda^4}$$

by a series of uniformly spaced gaussian striations. A reasonable approximation was obtained if  $\sigma_c^2 = \lambda_c^2/22$ . Alternatively, if the relationship is based upon either the sine wave or a series of gaussian striations which have equal maximum concentrations and produce the same rms scattering coefficient, the relationship should be  $\sigma_c^2 = \lambda_c^2/\pi^{3/2} = \lambda_c^2/17.5$ . Consequently, a ratio of the order of 20 is reasonable.

### 3. PROPAGATION ANALYSIS

#### 3.1 Random Walk Approach to Scattering

Inasmuch as the density of striations is relatively great, a particular ray will interact with several and exhibit motion that can be treated as a random walk (in angular deviation). The bending of a ray in an inhomogeneous medium is given by

$$\frac{d\theta}{dx} = \frac{\lambda}{2\pi} \frac{d}{dl} \left( \frac{d\phi}{dx} \right) , \quad (10)$$

where  $\frac{d}{dl}$  indicates a spatial derivative perpendicular to the direction of propagation. (Because the striations are extended along the geomagnetic field, the problem can be treated as two dimensional—all bending being in the plane normal to the geomagnetic field.)

Equations 7 and 8 can be used to obtain the deviation due to one gaussian striation. If the bending is great, system operation will fail. It follows that for cases of interest, the ray path will be nearly a straight line and the deflection can be approximated by integrating the incremental bending along a straight line. Let a particular sight line pass a distance  $b$  from the striation axis. Therefore,

$$\delta\theta(b) = \frac{\lambda}{2\pi} \int_{-\infty}^{\infty} \frac{d}{dl} \frac{d\phi}{dx} dx . \quad (11)$$

The integration and  $\frac{d}{dl}$  are independent, and their order can be reversed

$$\delta\theta(b) = \frac{\lambda}{2\pi} \frac{d}{dl} \int_{-\infty}^{\infty} \frac{d\phi}{dx} dx \quad (12)$$

$$= \frac{d}{dl} \int_{-\infty}^{\infty} \frac{n_0}{2n_c} dx \quad (13)$$

$$= \frac{d}{dl} \int_{-\infty}^{\infty} \frac{n_0}{2n_c} e^{-\frac{b^2 + (x - x_1)^2 \sin^2 \alpha}{2\sigma^2}} dx, \quad (14)$$

where the point of closest approach of the striation axis and the sight path is at  $x_1$  and  $\alpha$  is the angle between the sight path and the striation axis. The terminals of the path are sufficiently far from the striation axis that there is little error produced by placing the limits of integration at  $\pm\infty$ .

$$\delta\theta(b) = \frac{n_0 \sqrt{2\pi} \sigma}{2n_c \sin \alpha} \frac{d}{dl} e^{-b^2/2\sigma^2} \quad (15)$$

In this form the perpendicular derivative is the derivative with respect to  $b$  or

$$\delta\theta(b) = \frac{n_0 \sqrt{2\pi}}{2n_c \sin \alpha} \frac{b}{\sigma} e^{-b^2/2\sigma^2} \quad (16)$$

After a random walk, the final value tends toward a gaussian distribution with a variance equal to the sum of the squares of the individual steps. The value of the mean of this sum can be obtained by multiplying the

square of the incremental deviation (Equation 16) by the probability of having a striation of size  $\sigma$  at a displacement  $b$  and integrating over all  $\sigma$  and  $b$ . Thus,

$$\sigma_0^2 = \frac{\pi}{2n_c^2 \sin^2 \alpha} \int_{\sigma=0}^{\infty} \int_{b=-\infty}^{\infty} \frac{n_0^2 b^2}{\sigma^2} e^{-b^2/\sigma^2} P(\sigma) \sin \alpha mL \, d\sigma \, db \quad (17)$$

where  $m$  is the concentration of striations on a plane normal to their axes,  $L$  is the length of the path through the striated region and  $P(\sigma)$  is the probability density function of  $\sigma$ .

$$\sigma_0^2 = \frac{\pi^{3/2} mL}{4 n_c^2 \sin^2 \alpha} \int_{\sigma=0}^{\infty} n_0^2 \sigma^2 P(\sigma) \, d\sigma \quad (18)$$

We will use the notation

$$\overline{n_0^k \sigma^k} = \int_{\sigma=0}^{\infty} n_0^k \sigma^k P(\sigma) \, d\sigma \quad (19)$$

Thus, Equation 18 can be written

$$\sigma_0^2 = \frac{\pi^{3/2} mL}{4 n_c^2 \sin^2 \alpha} \frac{\overline{n_0^2 \sigma^2}}{n_0^2} \quad (20)$$

This equation allows the computation of the variance of the scattering, and after numerous scattering events, the distribution of power tends to a gaussian distribution. The gaussian character is the result of the multiplicity of events, not the distribution of angles due to a single interaction. Consequently, it is not a function of the electron profile in the striation. In fact, the scattering from a gaussian rod is far from gaussian but exhibits discrete maximum scattering angles each side of zero and has maximum probability at the extremes of the distribution.

The restriction on the applicability of this analysis is that all of the potential scatter paths contributing energy in a certain direction must be phase incoherent in order that interference patterns do not exist. As will be discussed later, for rms scattering in excess of a few milliradians, for typical structural dimensions and UHF radars, phase independence should be assured.

In one sense, the random walk analysis is the most general treatment in the strong scattering case. It is applicable even for environments that produce crossing of rays within the medium.

### 3.2 Phase Screen Approximation to Strong Scattering

The phase screen approximation to refraction and scattering assumes the scattering medium is sufficiently localized that its effect can be approximated by considering that all the phase shift experienced by a ray traversing the medium can be attributed to a thin screen in the middle of the medium. It also implies that the amplitude is constant over the screen. This section will cover parameters describing the screen and the relationship to volume characteristics of the medium.

Usually the characteristic assigned to the screen is the integral of the phase shift on a line parallel to the undisturbed ray. That is, if the radar is at  $-R_p, 0$  and the target is at  $R_T, 0$ ,

$$\phi(y) = \int_{-R_p}^{R_T} \frac{d\phi(x,y)}{dx} dx. \quad (21)$$

In the limit that the phase is the result of a random process and irregularities fill Fresnel zones, the angular deviation is

$$\theta = \frac{\lambda}{2\pi} \frac{d\phi}{dy}. \quad (22)$$

Close to the phase screen, these conditions are valid because Fresnel zones are small compared to the typical striation sizes of many hundreds of meters. Under these conditions, it is also possible to determine the power in the multipath rays by considering the region over which a wave is scattered coherently, i.e., the extent over which the "scattered ray" varies by only  $\lambda/2$ . This is controlled by the second derivative of the phase shift.

Let us first develop expressions relating the phase shift to plasma parameters and then determine the scattering. Then the scattering will be discussed in terms of the characteristics of the energy at the radar.

The mean integrated electron content associated with the striations is obtained by forming the product of the probability that a striation axis lies at some impact parameter and the integral of electron content for that striation and impact parameter, and integrating the product over all impact parameters.\*

$$\bar{N} = \int_0^{\infty} \int_{-\infty}^{\infty} \int_{-\infty}^{\infty} n_0 e^{-\frac{(b^2 + x^2 \sin^2 \alpha)}{2\sigma^2}} \sin \alpha m P(\sigma) L dx db d\sigma \quad (23)$$

$$= 2\pi mL n_0^{-1} \sigma^2 . \quad (24)$$

The contribution of the striations to the local electron concentration is just  $\bar{N}/L$ . The striations normally are superimposed upon a constant (or

---

\* The limits of  $\pm\infty$  on the  $x$  integral reflect the assumption that the striation sizes  $\sigma$  are small compared to  $L$  so that little error results in extending the limits of integration rather than truncating them at their actual value.

slowly varying) concentration  $n_0^*$  that may be considerably greater than the mean striation contribution. The total mean electron concentration is

$$\bar{n}_e = n_0^* + \bar{N}/L . \quad (25)$$

A parameter some plasma physicists feel they can compute is the local mean-square electron concentration fluctuation due to striation structure.

$$\begin{aligned} \sigma_n^2 &= \overline{n_e^2} - \bar{n}_e^2 \\ &= \int_0^\infty \int_0^\infty n_0^2 e^{-\frac{r^2}{\sigma^2}} 2\pi r \sin^2(\sigma) dr d\sigma - (\bar{N}/L)^2 \end{aligned} \quad (26)$$

$$= \pi n_0^2 \overline{\sigma^2} - (\bar{N}/L)^2 \quad (27)$$

In the remainder of this report the term  $(\bar{N}/L)^2$  will be dropped, an approximation valid for striations sufficiently separated that the primary contribution to  $\sigma_n^2$  is from regions without striation overlap (i.e.  $4\pi n_0^2 \sigma^2 \ll 1$ ).

The mean phase shift through the screen is unimportant to the problem being addressed but could be easily obtained from Expression 25.

In the following, the direction of primary propagation (the sight path) is nearly parallel to the x-axis, the striation axes lie parallel to a line in the x-z plane that makes an angle  $\alpha$  relative to the x-axis, and the coordinate y is perpendicular to both the sight path and the striation axes. Moreover, any fixed background of electron content not associated with striations has been suppressed because it does not affect the scattering and is accounted for in refraction calculations.

The variance of phase shift is important because it determines the magnitude of phase shift fluctuations. Consider a particular striation with its axis at  $y = b_1$ . The integrated phase shift along the line  $y = 0$  is

$$\delta\phi_1 = \frac{\pi n_1}{\lambda n_c} \int_{-\infty}^{\infty} \exp\left[-\frac{(b_1^2 + x^2 \sin^2 \alpha)}{2\sigma_1^2}\right] dx \quad (28)$$

$$= \frac{\sqrt{2\pi} \pi n_1 \sigma_1}{\lambda n_c \sin \alpha} e^{-b_1^2/2\sigma_1^2} \quad (29)$$

Let  $C = \frac{\sqrt{2\pi} \pi}{\lambda n_c \sin \alpha}$  and  $p_1 = n_1 \sigma_1$ .

The phase shift variance is

$$\sigma_\phi^2 = \overline{\phi^2} - \bar{\phi}^2 \quad (30)$$

where  $\phi$  is a sum over all striations, or

$$\sigma_\phi^2 = C^2 \left[ \overline{\sum_1 p_1 \exp(-b_1^2/2\sigma_1^2)} \right]^2 - \bar{\phi}^2 \quad (31)$$

The bar designates an average over all possible configurations of striations. This can be rewritten

$$\begin{aligned} \sigma_\phi^2 = C^2 & \left[ \overline{\sum_1 p_1^2 \exp(-b_1^2/\sigma_1^2)} \right] \\ & + C^2 \overline{\sum_1 \sum_{j \neq 1} p_1 p_j \exp(-b_1^2/2\sigma_1^2 - b_j^2/2\sigma_j^2)} - \bar{\phi}^2. \quad (32) \end{aligned}$$

The assumption that the striations are randomly located implies that  $b_1$  is independent of  $b_j$  so that the mean of a product of functions of  $i$  and  $j$  equals the product of the individual means, or

$$\sigma_{\phi}^2 = c^2 \overline{\sum p_i^2 \exp(-b_i^2/\sigma_i^2)} - \bar{\phi}^2 + c^2 \overline{\sum_i p_i \exp(-b_i^2/2\sigma_i^2) \sum_{j \neq i} p_j \exp(-b_j^2/2\sigma_j^2)} \quad (33)$$

The last term in Equation 33 is made up of two factors, the first is  $\bar{\phi}$  and the second  $\bar{\phi} (1 - \frac{1}{k})$  where  $k$  is the number of striations. If  $k$  is large, the  $1/k$  will be negligible, and it will be so assumed here. Thus

$$\sigma_{\phi}^2 = c^2 \overline{\sum_i p_i^2 \exp(-b_i^2/\sigma_i^2)} \quad (34)$$

For large ensembles, the summation and averaging can be approximated by integrating over the spatial and size distribution functions\*

$$\sigma_{\phi}^2 = c^2 \int_0^{\infty} \int_{-\infty}^{\infty} n_{\delta}^2 \sigma^2 \exp(-b^2/\sigma^2) mL \sin \alpha P(\sigma) db d\sigma \quad (35)$$

$$= \frac{2\pi^{3/2} mL}{\lambda^2 n_c^2 \sin \alpha} \overline{n_{\delta}^2 \sigma^3} \quad (36)$$

The factor  $\sin \alpha$  occurs in Equation 35 because the concentration of striations in the  $xy$  plane is  $m \sin \alpha$ .

---

\* The result, Equation 36, can be combined with Equation 27 to give

$$\sigma_{\phi}^2 = \frac{2\pi^{3/2} \sigma_{\text{eff}}^4}{\lambda^2} \frac{\sigma_n^2}{n_c^2} \quad \text{where} \quad \sigma_{\text{eff}} = \overline{n_{\delta}^2 \sigma^3 / n_{\delta}^2 \sigma^2}. \quad \text{This is the same}$$

form derived by Bramley<sup>(4)</sup> for a thick scattering region.

Another function, useful because it determines the scattering, is the autocorrelation function of the phase shift. It can be computed in a manner similar to that used for the variance of phase. The normalized autocorrelation function is defined as

$$R(\xi) = \frac{[\phi(y) - \bar{\phi}][\phi(y+\xi) - \bar{\phi}]}{\sigma_{\phi}^2} \quad (37)$$

$$= \frac{\phi(y) \phi(y+\xi) - \bar{\phi}^2}{\sigma_{\phi}^2} \quad (38)$$

$$= \frac{C^2}{\sigma_{\phi}^2} \left[ \sum_1 p_1 \exp\left(-\frac{(y-b_1)^2}{2\sigma_1^2}\right) \right] \left[ \sum_1 p_1 \exp\left(-\frac{(y+\xi-b_1)^2}{2\sigma_1^2}\right) \right] - \bar{\phi}^2 \quad (39)$$

(R will be used to denote various autocorrelation functions but when unsubscripted will denote the phase autocorrelation function.) By a sequence of steps analogous to those in Equations 31 through 34, Equation 39 can be reduced to

$$R(\xi) = \frac{C^2}{\sigma_{\phi}^2} \sum_1 p_1^2 \exp\left(-\frac{(y-b_1-\xi/2)^2}{\sigma_1^2}\right) \exp\left(-\frac{\xi^2}{4\sigma_1^2}\right). \quad (40)$$

Again, the average of the sum can be approximated by an integral over space and striation parameter.

$$R(\xi) = \frac{2\pi^{7/2} mL}{\lambda^2 n^2 \sin \alpha \sigma_\phi^2} \int_0^\infty n_0^2 \sigma^3 \exp\left(-\frac{\xi^2}{4\sigma^2}\right) P(\sigma) d\sigma \quad (41)$$

Or, if the value of  $\sigma_\phi^2$  is substituted from Expression 36,

$$R(\xi) = \frac{\int n_0^2 \sigma^3 \exp(-\xi^2/4\sigma^2) P(\sigma) d\sigma}{n_0^2 \sigma^3} \quad (42)$$

How does this relate to ray deviation? Consider the general normalized autocorrelation function where for simplification in writing  $\phi$  is taken as the deviation from the mean.

$$R(\xi) = \lim_{y_1 \rightarrow \infty} \left\{ \int_{-y_1}^{y_1} \phi(y) \phi(y + \xi) dy \right\} / 2y_1 \sigma_\phi^2 \quad (43)$$

The second derivative of  $R(\xi)$  at  $\xi = 0$  is

$$R''(0) = \lim_{y_1 \rightarrow \infty} \left\{ \int_{-y_1}^{y_1} \phi(y) \phi''(y) dy \right\} / 2y_1 \sigma_\phi^2 \quad (44)$$

Integrate this by parts once to obtain

$$R''(0) = \lim_{y_1 \rightarrow \infty} \left\{ \frac{\phi(y) \phi'(y)}{2y_1 \sigma_\phi^2} \Big|_{-y_1}^{y_1} - \frac{1}{2y_1 \sigma_\phi^2} \int_{-y_1}^{y_1} [\phi'(y)]^2 dy \right\} \quad (45)$$

If  $\phi$  and  $\phi'$  remain small over the range of interest, the first term of the right hand member becomes small compared to the second. Moreover, the second term is the ratio of the variances of the derivative of phase and the phase. Consequently,

$$\sigma_{\phi'}^2 = -\sigma_{\phi}^2 R''(0) \quad , \quad (46)$$

( $\phi'$  is assumed to have zero mean).

The deviation is directly related to the derivative of phase shift (Equation 22). Thus,

$$\sigma_{\theta}^2 = \frac{\lambda^2}{4\pi^2} \sigma_{\phi'}^2 = -\frac{\lambda^2 \sigma_{\phi}^2}{4\pi^2} R''(0) \quad . \quad (47)$$

As used here  $\sigma_{\theta}^2$  is the variance of ray bending or scattering angle. In later analyses, it loses that physical significance but is still a useful characterization parameter for the plasmas. This can be used with Expression 41 to give

$$\sigma_{\theta}^2 = \frac{\pi^{3/2} \text{ml.}}{4 \sin \alpha n_c^2} \overline{n_0^2 \sigma} \quad , \quad (48)$$

which is identical to the result given in Equation 20.

### 3.3 Ray Optics and Stationary Phase Analysis

#### 3.3.1 Scattering as Viewed by the Radar

The geometry of the thin phase screen-radar-target is shown in Figure 1. Up until now the scattering angle  $\theta$  has been discussed. It can be seen that the angle of scatter seen by the radar  $\psi$  is

$$\psi = \theta R_T / (r + R_T) \quad (49)$$

if the angles are small.

In the strong scattering case (the phase screen having many radians phase shift), unless there is a region of the screen for which the scatter path phase shift is constant, the scattered energy will add incoherently and contribute a noise-like, random phase background. The scattered waves from regions of constant or stationary phase will combine coherently and form discrete scatter ray paths.

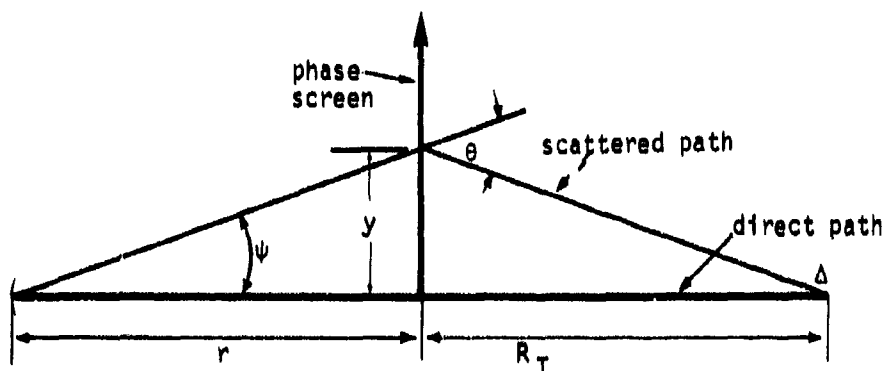


Figure 1. Scatter geometry.

The total phase advance including geometric and phase screen contributions for a path penetrating the screen at  $y$  is (for small angles,)

$$\phi_T = -\frac{\pi y^2}{\lambda R} + \phi, \quad (50)$$

where

$$R^{-1} = r^{-1} + R_p^{-1}, \quad (51)$$

Fermat's principle leads to the condition that rays between two points (radar and target) propagate over paths of local extreme phase deviation, i.e., where the derivative of phase is zero. These are called points of stationary phase. If we set the derivative of  $\phi_T$  equal to zero, we get

$$\phi'(y_1) = y_1/f, \quad (52)$$

where  $f$  has been used to represent  $\lambda R/2\pi$ . Equations 49 and 52 represent the same relationship if  $\theta = \frac{\lambda}{2\pi} \phi'$ , which was previously derived as the scattering angle at the phase screen.

The intensity from one of these regions is determined by the extent of the coherence region. The amplitude varies as the linear extent, the power as the square of the extent. Quantitatively, the extent will be about that for which  $|\Delta\phi_T| < \pi$ . That is,

$$|\phi_T(y) - \phi_T(y_1)| = \pi = \left| -\frac{y^2 - y_1^2}{2f} + \phi'(y_1) \Delta y + \phi''(y_1) \frac{\Delta y^2}{2} \right|, \quad (53)$$

where the phase shift has been expanded as a Taylor series truncated after the quadratic term and  $\Delta y = y - y_1$ . Algebraic manipulation of this using the value of  $\phi'$  from Equation 52 produces

$$\Delta y^2 = 2\pi \left| \frac{1}{f} - \phi''(y_1) \right|^{-1}. \quad (54)$$

For no striations or refraction,  $\phi''$  is zero everywhere. The use of this normalizes Equation 54 to the undisturbed power gain.

$$\frac{P}{P_0} = \frac{1}{1 - f\phi''(y_1)} \quad (55)$$

Although Equation 55 indicates that  $P/P_0$  could go to infinity if  $f\phi'' = 1$ , this is a fallacy introduced by dropping high-order derivatives from Equation 53. If the structure of the phase screen has a characteristic dimension  $\ell$  and scattering is strong, it is unlikely that the phase is "stationary" for more than a distance  $\ell/10$ . If this is used to estimate an upper limit on the power gain,

$$\frac{P_m}{P_0} = \frac{\ell^2}{200\pi f} = \frac{\ell^2}{100\lambda R} \quad (56)$$

The analysis in this section does not require that the regions of stationary phase be as large as a Fresnel zone ( $\ell_f^2 = \lambda R$ ), but it is apparent from Equation 56 that the power gain on a ray path is the square of the extent of coherence measured in terms of the first Fresnel zone size. Consequently, if the structure is fine, most of the energy is either scattered out of the beam or combines noncoherently.

### 3.3.2 Distribution in Phase, Angle and Power

The random walk analysis leads one to believe that the angular scattering distribution should tend toward a gaussian distribution. Does the stationary phase analysis give the same answer? And if so, can one draw conclusions about the distribution of phase shifts and amplitudes? The answer is yes.

If a straight path through the medium intersects many randomly placed striations, the number intersected will have a Poisson distribution, which approximates a gaussian for large numbers of intersections. Consequently, in this limit  $\phi(y)$  is gaussianly distributed.

Call its normalized autocorrelation function  $R(\xi)$ . This means that if the phase screen is randomly sampled at points sufficiently spaced that  $R(\xi) \ll 1$ , the values so measured will form a gaussian distribution with variance  $\sigma_\phi^2$ , as already computed.

For such a random gaussian sequence, samples spaced  $\Delta y$  apart, satisfy the relationship

$$\phi(y+\Delta y) = \phi(y) R(\Delta y) + \sqrt{1-R^2(\Delta y)} g\sigma_\phi, \quad (57)$$

where  $g$  is a gaussian variate from a unit variance distribution. This allows the computation of the derivative of  $\phi$ ,

$$\frac{d\phi}{dy} = \phi' = \lim_{\Delta y \rightarrow 0} \frac{\phi(y+\Delta y) - \phi(y)}{\Delta y} \quad (58)$$

To evaluate this derivative requires knowing  $R(\xi)$  only near the origin. As was previously shown (Equation 46), for well behaved sequences, the autocorrelation function is parabolic near the origin. Thus,

$$R(\xi) = 1 - \frac{\sigma_{\phi'}^2}{\sigma_\phi^2} \frac{\xi^2}{2} = 1 - a\xi^2/2, \quad (59)$$

a just being used for  $\sigma_{\phi'}^2/\sigma_\phi^2$  for convenience.

The combination of Equations 57, 58 and 59 yields

$$\phi' = \lim_{\Delta y \rightarrow 0} \frac{\phi - a\Delta y^2 \phi/2 + \sqrt{a\Delta y^2} g\sigma_\phi - \phi}{\Delta y} \quad (60)$$

$$= \sqrt{a} g\sigma_\phi = \sigma_{\phi'} g \quad (61)$$

It is evident that the gaussian character of the  $\phi$  distribution is adequate to guarantee a gaussian distribution of  $\phi'$ . Intuitively we suspect that the conditions necessary to produce a gaussian  $\phi$  distribution are those necessary to produce a gaussian distribution in the random walk.

The other, very significant implication of Equation 61 is that the slope of the curve  $\phi'$  is independent of the value of  $\phi$ . This means that at points of stationary phase, the phase shift  $\phi$  is not related to the deflection which is determined by  $\phi'$  but rather is independently gaussianly distributed with its own variance  $\sigma_\phi^2$ . Consequently, so long as  $\sigma_\phi \gg 1$ , the phases of the various rays are indeed uncorrelated.

The proper gaussian statistics for  $\phi$  and correlation between samples are maintained for three equally spaced samples if the second is determined by Equation 57 and the third is determined by

$$\begin{aligned} \phi(y+2\Delta y) = & \frac{R(2\Delta y) - R^2(\Delta y)}{D} \phi(y) + \frac{R(\Delta y)[1-R(2\Delta y)]}{D} \phi(y+\Delta y) \\ & + \sqrt{\frac{1 + 2R^2(\Delta y)R(2\Delta y) - 2R^2(\Delta y) - R^2(2\Delta y)}{D}} g\sigma_\phi. \end{aligned} \quad (62)$$

where  $D = 1 - R^2(\Delta y)$  (Reference 5).

This can be used with the autocorrelation function to compute the second derivative

$$\phi''(y) = \lim_{\Delta y \rightarrow 0} \frac{\phi(y+2\Delta y) - 2\phi(y+\Delta y) + \phi(y)}{\Delta y^2}; \quad (63)$$

however, terms of higher order than  $\epsilon^2$  must be carried in the autocorrelation function in order to properly represent the first significant term in the radical of Equation 62.

The necessary expression for the autocorrelation function is

$$R(\xi) = 1 - a\xi^2/2 + b\xi^4/24 \quad (64)$$

The coefficient  $b$  is

$$b = \left. \frac{d^4 R}{d\xi^4} \right|_0 \equiv R_{\phi}^{IV}(0) \quad (65)$$

This can be obtained by taking the derivative with respect to  $\xi$  of Equation 41 and then setting  $\xi = 0$ . Thus

$$R_{\phi}^{IV}(0) = \frac{\frac{3}{4} \frac{n\delta^2 \sigma^{-1}}{n\delta \sigma^3}}{\quad} \quad (66)$$

By taking the fourth derivative of the general equation for the autocorrelation function (Equation 42) and integrating by parts twice, we also obtain

$$R_{\phi}^{IV}(0) = \frac{\phi''^2}{\sigma_{\phi}^2} \quad (67)$$

These will allow the determination of the second derivative correlation when Equation 63 is evaluated.

The evaluation of Equation 63 using expressions 57, 62 and 63 is straightforward algebra, but tedious. The result is

$$\phi'' = -a\phi + \sqrt{b-a^2} g\sigma_{\phi} \quad (68)$$

$$= -\frac{\sigma_{\phi'}^2}{\sigma_{\phi}^2} \phi + \sqrt{1 - \frac{\sigma_{\phi'}^4}{\sigma_{\phi}^2 \sigma_{\phi''}^2}} g\sigma_{\phi''} \quad (69)$$

The implication of Equation 69 is that the second derivative of  $\phi$ , which determines the strength of a multipath ray, is correlated with the phase shift on that ray and has a random component as well. Because there is no correlation between the phase shift and the first derivative, it follows that there is also none between the first and second derivative (a result of its dependence on  $\phi$  itself). The same independence can be proven because the first derivative is a gaussian sequence similar to  $\phi$  according to Equation 62, and consequently its derivative is uncorrelated with itself.

The deductions from these correlation analyses are that at any point on the phase screen,  $\phi'$  is gaussianly distributed, and hence the probability of a stationary phase ray occurring at a particular value of  $y$  is a gaussian function of  $y$  in order that relationship Equation 52 is satisfied. The phase screen phase shift along a ray path is also gaussianly distributed and uncorrelated with the scattering angle. The second derivative of the phase shift which determines the strength of the signal propagated along a ray is also gaussianly distributed, being the weighted sum of two gaussian variates —  $\phi$  and  $g$ . The intensity of a ray is uncorrelated with the angular deviation because  $\phi'$  and  $\phi''$  are uncorrelated — all possible paths have the same energy probability distribution function. Consequently, because the number of paths varies gaussianly with angle, the total power scattered varies gaussianly with angle.

### 3.3.3 Density of Multipath Returns

Previous analysis <sup>(6)</sup> has shown that when multipath scattering conditions exist, if consideration is taken of all the combinations of outgoing and return paths, the number of combination rays becomes

very large. They are typically spaced at effective range separations of a fraction of a meter over a region with a variance

$$\sigma_L^2 \approx \frac{\lambda^2}{4\pi^2} \left[ \frac{f^2}{4} \sigma_{\phi_1}^4 + \frac{g^2}{4\pi} \sigma_{\phi_1}^2 \right] \quad (70)$$

If the radar is not an extremely short pulse system, many signals that appear randomly phased will interact in the monopulse processor as was assumed in the original HARC analysis. Consequently, that analysis which assumed the combination of randomly phased vectors in the sum and difference channels of a monopulse processor is indeed valid for the strong scattering case.

The sensitivity of radar output to variations in environmental models will be discussed later. The extension of the theory to the generalized physical optics case will be discussed next.

### 3.4 Huygens' Wave Theory and Angular Power Spectrum

Huygens' wave formulation is that at a particular instant in time one may consider a new spherically divergent wave starts at every point on a wave front. The superposition of these wavelets is the solution to the wave equation at a future point in time. This formulation is, in fact, the basis for the analysis of the previous section where the regions of stationary phase imply that the wavelets add coherently.

In this section, the initial wave will be assumed to be a plane wave, there will be a phase shift introduced by a thin phase screen, the angular region of interest will be limited to nearly forward scatter so that the wavelet amplitude is independent of angle, and the angular spectrum will be analyzed far from the screen so the range to the screen is nearly independent of position (from the

standpoint of power divergence, not phase shift). The angular power spectrum will be obtained for limiting cases of large and small phase perturbations and, for one striation distribution, for all phase perturbations.

Booker<sup>(7)</sup> has shown that the angular distribution of power scattered by a plane wave incident on a plane phase screen can be obtained as

$$P(\theta) = \frac{P_0}{\lambda} \int_{-\infty}^{\infty} R_E(\xi) e^{-i \frac{2\pi\theta\xi}{\lambda}} d\xi \quad (71)$$

where  $R_E(\xi)$  is the autocorrelation function of the electric field and  $P_0$  is the integral of  $P(\theta)$  over all  $\theta$ . Equation 71 is valid in regions where  $\sin\theta \approx \theta$  — i.e. most energy scattered at small angles.

### 3.4.1 Autocorrelation Function of Electric Field

The autocorrelation function of the electric field is

$$R_E(\xi) = \overline{E(y) E^*(y+\xi)}, \quad (72)$$

where the asterisk denotes the complex conjugate and the field strengths are normalized to unity. Consequently,

$$R_E(\xi) = \overline{\exp[i\phi(y) - i\phi(y+\xi)]}. \quad (73)$$

The phase shift at  $y+\xi$  can be expressed in terms of the phase autocorrelation function as given in Equation 57.

$$R_E(\xi) = \overline{\exp \left\{ i \phi(y) [1-R(\xi)] - i \sqrt{1-R(\xi)^2} g \sigma_\phi \right\}} . \quad (74)$$

Inasmuch as  $\phi(y)$  and  $g$  are independent, the average in Equation 74 can be obtained by multiplying by each distribution function and integrating over  $\phi(y)$  and  $g$ . This yields

$$\begin{aligned} R_E(\xi) &= \frac{1}{\sqrt{2\pi}\sigma_\phi} \int \exp \left\{ i \phi(y) [1-R(\xi)] - \phi^2(y)/2\sigma_\phi^2 \right\} d\phi(y) \\ &\times \frac{1}{\sqrt{2\pi}} \int \exp \left\{ -i \sqrt{1-R(\xi)^2} g \sigma_\phi - g^2/2 \right\} dg . \end{aligned} \quad (75)$$

This is integrable by the technique shown in Appendix A.

$$R_E(\xi) = \exp \left\{ -\sigma_\phi^2 [1-R(\xi)]^2/2 - \sigma_\phi^2 [1-R(\xi)^2]/2 \right\} \quad (76)$$

$$= \exp \left\{ -\sigma_\phi^2 [1-R(\xi)] \right\} , \quad (77)$$

which is exactly that relationship derived by Bramley<sup>(4)</sup>. This expression can now be used in Equation 71 to obtain the angular power spectrum.

### 3.4.2 Unmodified Components

The expression for the power spectrum can be written in a slightly different form

$$P(\theta) = \lim_{x \rightarrow \infty} \frac{P_\theta}{\lambda} \int_{-x}^x \exp \left\{ -\sigma_\phi^2 [1-R(\xi)] - i 2\pi\theta\xi/\lambda \right\} d\xi . \quad (78)$$

The approximation will be used that the autocorrelation function can be reasonably represented (reference Equation 59) by

$$R(\xi) = \begin{cases} 1 - \xi^2 \sigma_{\phi_1}^2 / 2\sigma_{\phi}^2 & \text{if } \xi < \xi_1 \\ 0 & \text{if } \xi \geq \xi_1 \end{cases} \quad (79)$$

where  $\xi_1 = \sqrt{2} \sigma_{\phi} / \sigma_{\phi_1}$ . Insert this in Equation 78.

$$P(\theta) = \frac{P_0}{\lambda} \int_{-\xi_1}^{\xi_1} \exp[-\xi^2 \sigma_{\phi_1}^2 / 2 - i 2\pi\theta\xi/\lambda] d\xi \\ + \lim_{x \rightarrow \infty} \frac{2P_0}{\lambda} \int_{\xi_1}^x \exp(-\sigma_{\phi}^2) \cos(2\pi\theta\xi/\lambda) d\xi \quad (80)$$

$$P(0) = \frac{P_0}{\lambda} \int_{-\xi_1}^{\xi_1} \exp[-\xi^2 \sigma_{\phi_1}^2 / 2 - i 2\pi\theta\xi/\lambda] d\xi \\ + P_0 \lim_{x \rightarrow \infty} \left\{ \exp(-\sigma_{\phi}^2) \frac{\sin 2\pi\theta x/\lambda - \sin 2\pi\theta\xi_1/\lambda}{\pi\theta} \right\} \quad (81)$$

Expression 81 will be used to determine the unmodified signal penetrating the scattering medium and the scattered signal for  $\sigma_{\phi} \gg 1$ .

### 3.4.3 Unmodified Signal

The second term of Expression 81 gives the unmodified or direct component  $P_u$ . For  $\theta = 0$ , this term gives

$$P_u = 2P_0 \lim_{x \rightarrow \infty} \left\{ \exp(-\sigma_\phi^2) \frac{x - \xi_1}{\lambda} \right\} , \quad (82)$$

which approaches an infinite angular power density. Of course, the incident plane wave had an infinite angular power density there. However, if we perform an integral over  $\theta$  before letting  $x \rightarrow \infty$ , we will obtain the power in the unmodified beam. (This power is concentrated in an angular width of the order of  $\lambda/x$ , which accounts for the constant unscattered power flux as  $x \rightarrow \infty$ .) To accomplish this, redefine  $P_u$  as

$$P_u = P_0 \lim_{x \rightarrow \infty} \int_{-\theta_d}^{\theta_d} \exp(-\sigma_\phi^2) \frac{\sin 2\pi\theta x/\lambda - \sin 2\pi\theta \xi_1/\lambda}{\pi\theta} d\theta . \quad (83)$$

The direct beam will be defined as being in that angular width  $\theta_d$  such that  $2\pi\theta_d x/\lambda \gg 1$  and  $2\pi\theta_d \xi_1/\lambda \ll 1$ . This is equivalent to restricting the geometry such that the scattering medium is at least several decorrelation widths wide. With this restriction

$$P_u = P_0 e^{-\sigma_\phi^2} \lim_{x \rightarrow \infty} \left\{ \int_{-\infty}^{\infty} \frac{\sin 2\pi\theta x/\lambda}{\pi\theta} d\theta - \int_{-\theta_d}^{\theta_d} \frac{2\xi_1}{\lambda} d\theta \right\} \quad (84)$$

$$= P_0 e^{-\sigma_\phi^2} . \quad (85)$$

The last term in Equation 84 is negligible based upon the restriction  $2\pi\theta_d \xi_1/\lambda \ll 1$ . Consequently, the direct unmodified component is always  $e^{-\sigma_\phi^2}$  times the incident power and can be represented by

$$P_u = P_0 e^{-\sigma_\phi^2} \delta(\theta), \quad (86)$$

where  $\delta(\theta)$  is a delta function.

#### 3.4.4 Large Phase Perturbation Scattered Signal

If the phase perturbation  $\sigma_\phi$  is large

$$\xi_1 \sigma_\phi / \sqrt{2} = \sigma_\phi \gg 1, \quad (87)$$

and in Equation 81, the limits of integration can be extended to infinity with little error. Integrating this term according to the means of Appendix A gives

$$P_1(\theta) = \frac{P_0}{\sqrt{2\pi} \sigma_\theta} e^{-\frac{\theta^2}{2\sigma_\theta^2}} \quad (88)$$

a normal distribution with variance  $\sigma_\theta^2$ . It can be noted that as it stands, the integral of  $P_1$  over  $\theta$  is  $P_0$ , the total incident power.

The term involving the limit on  $x$  is already accounted for in the unscattered beam.

The final term in Equation 81, involving  $\sin(2\pi\theta\xi_1/\lambda)$ , can slightly add or subtract from the scattered component but on the average subtracts and, indeed, when integrated over  $\theta$ , removes from the scattered beam exactly the amount of power that is in the unscattered beam. Its magnitude is always less than 20 percent of the main scattered component and, for values of  $\sigma_\phi$  in excess of about 2, is less than 1 percent.

Consequently, little error is introduced, calculations are simplified and energy is conserved, if the average correction due to the last term is used for all angles. That is, the power distribution of Equation 88 is multiplied by  $1 - \exp(-\sigma_\phi^2)$ .

Using this last approximation, the total power angular distribution function for the case  $\sigma_\phi \gg 1$  can be written

$$P(\theta) = P_0 \left\{ e^{-\sigma_\phi^2} \delta(\theta) + \frac{(1 - e^{-\sigma_\phi^2})}{\sqrt{2\pi} \sigma_\theta} e^{-\frac{\theta^2}{2\sigma_\theta^2}} \right\} . \quad (89)$$

### 3.4.5 Small Phase Variance Scattered Signal

To investigate the case of small phase variance, it is more instructive to return to the basic expression for the angular power spectrum, Equation 78, and expand the exponential:

$$e^{-\sigma_\phi^2 [1 - R(\xi)]} \approx e^{-\sigma_\phi^2} + (1 - e^{-\sigma_\phi^2}) R(\xi) . \quad (90)$$

When the approximation of Equation 90 is used in Equation 71, the integral of the first term leads to the delta function, and

$$P(\theta) = P_0 \left\{ e^{-\sigma_\phi^2} \delta(0) + 2 \frac{1 - e^{-\sigma_\phi^2}}{\lambda} \int_0^\infty R(\xi) \cos(2\pi\theta\xi/\lambda) d\xi \right\} . \quad (91)$$

At this point it becomes obvious that for this weak scattering case, the angular spectrum is not necessarily gaussian. That the spectrum was

gaussian for strong scattering was a result of  $\sigma_\phi^2[1 - R(\xi)]$  being large before terms in  $R(\xi)$  greater than quadratic were important. For weak scattering, a broader portion of the autocorrelation function will be significant. As examples, let us consider a medium of uniform gaussian rods and one following the experimental distribution function of Equation 9.

For a medium of uniform striations the autocorrelation function is

$$R(\xi) = \exp[-\xi^2/4\sigma^2] \quad (92)$$

( $P(\sigma)$  in Equation 42 is  $\delta(\sigma)$ .) This can be expressed in terms of the variance of phase and phase gradient by making use of the relationship  $R''(0) = -\sigma_\phi^2/\sigma_\phi^2$  and Equation 47:

$$R''(0) = -\frac{1}{2\sigma^2} = -\frac{\sigma_\phi^2}{\sigma_\phi^2} \quad (93)$$

When this is used in Expression 92 and the result inserted in Equation 91, the result is

$$P(\theta) = P_0 \left\{ e^{-\sigma_\phi^2} \delta(\theta) + \left(1 - e^{-\sigma_\phi^2}\right) \frac{\sigma_\phi}{\sqrt{2\pi} \sigma_0} e^{-\frac{1}{2} \left(\frac{\theta \sigma_\phi}{\sigma_0}\right)^2} \right\} \quad (94)$$

In this case the scattering does happen to be gaussian, but with an angular variance increased from  $\sigma_0^2$  to  $\sigma_0^2/\sigma_\phi^2$ .

For the experimentally derived Chesnut distribution, the autocorrelation function is

$$R(\xi) = \frac{1}{1 + (a\xi)^2} \quad (95)$$

or

$$R(\xi) = \frac{1}{1 + \frac{1}{2} \left( \frac{\sigma_{\phi'} \xi}{\sigma_{\phi}} \right)^2} \quad (96)$$

This can also be integrated explicitly in Equation 91. The result is

$$P(\theta) = P_0 \left\{ e^{-\sigma_{\phi}^2} S(\theta) + \left( 1 - e^{-\sigma_{\phi}^2} \right) \frac{\sigma_{\phi}}{\sqrt{\pi} \sigma_{\theta}} e^{-\frac{\sqrt{2} \sigma_{\phi} \theta}{\sigma_{\theta}}} \right\} \quad (97)$$

In this case the distribution is exponential, not gaussian, but there is little power in the scattered component because  $\sigma_{\phi}^2$  is assumed to be small.

#### 3.4.6 Variance of Angle of Arrival for Uniform Striations

For weak scattering, the energy is more broadly spread than defined by the parameter  $\lambda \sigma_{\phi} / 2\pi$ , which has been denoted  $\sigma_{\theta}$ . The spread is increased by a factor of the order of  $1/\sigma_{\phi}$ . For the uniform gaussian striation model the variance of the scattered power can be computed explicitly for all  $\sigma_{\phi}$ . To accomplish this, the exponential in Equation 78 can be expanded in a Taylor series and the result integrated term by term. Thus, because  $R(\xi) = \exp(-\xi^2/4\sigma^2)$ ,

$$P(\theta) = \frac{2P_0}{\lambda} e^{-\sigma_{\phi}^2} \int_0^{\infty} \left[ 1 + \sum_{n=1}^{\infty} \frac{1}{n!} \sigma_{\phi}^{2n} e^{-\frac{n\xi^2}{4\sigma^2}} \right] \cos(2\pi\theta\xi/\lambda) d\xi \quad (98)$$

The integral of the first (constant) term in the brackets is the direct unscattered beam. The scattered power is distributed

$$P_s(\theta) = \frac{2P_0}{\lambda} e^{-\sigma^2} \sum_{n=1}^{\infty} \frac{\sqrt{\pi}}{2} \frac{2\sigma}{\sqrt{n}} \frac{\sigma^{2n}}{n!} e^{-\frac{1}{n} \left( \frac{2\pi\theta\sigma}{\lambda} \right)^2} \quad (99)$$

as was obtained by Ratcliffe<sup>(8)</sup>. The variance of the scattered power is

$$\frac{\overline{\theta^2}}{\theta^2} = \frac{\int_0^{\infty} \theta^2 P_s(\theta) d\theta}{\int_0^{\infty} P_s(\theta) d\theta} \quad (100)$$

The integral can start at 0 because the distribution is symmetric about  $\theta = 0$ , and go to  $\infty$  because  $P_s$  is essentially zero beyond some value of  $\theta$ . This gives

$$\frac{\overline{\theta^2}}{\theta^2} = \frac{\sum_{n=1}^{\infty} \frac{\sigma^{2n}}{n! \sqrt{n}} \int_0^{\infty} \theta^2 e^{-\frac{1}{n} \left( \frac{2\pi\theta\sigma}{\lambda} \right)^2} d\theta}{\sum_{n=1}^{\infty} \frac{\sigma^{2n}}{n! \sqrt{n}} \int_0^{\infty} e^{-\frac{1}{n} \left( \frac{2\pi\theta\sigma}{\lambda} \right)^2} d\theta} \quad (101)$$

$$= \frac{\sum_{n=1}^{\infty} \frac{\sigma^{2n}}{n! \sqrt{n}} \left( \frac{n\lambda^2}{4\pi^2\sigma^2} \right)^{3/2}}{2 \sum_{n=1}^{\infty} \frac{\sigma^{2n}}{n! \sqrt{n}} \left( \frac{n\lambda^2}{4\pi^2\sigma^2} \right)^{1/2}} \quad (102)$$

$$= \frac{\lambda^2 \sigma^2}{8\pi^2 \sigma^2} \frac{\sum_{n=0}^{\infty} \frac{\sigma^{2n}}{n!}}{\left[ \sum_{n=0}^{\infty} \frac{\sigma^{2n}}{n!} - 1 \right]} \quad (103)$$

$$\overline{\theta^2} = \frac{\lambda^2 \sigma_\phi^2}{8\pi^2 \sigma^2} \frac{1}{1 - \exp(-\sigma_\phi^2)} \quad (104)$$

Although it is clear by inspection of Equation 99 that even for the homogeneous striation environment the power distribution is not gaussian for  $\sigma_\phi \approx 1$ , for radar modeling purposes, the correct character to the signal can probably be obtained by use of a gaussian distribution with a variance given by Equation 104. The striation parameter  $\sigma$  can be taken as an effective size. Both the impact of the distribution on the radar monopulse system and the choice of an effective size will be treated in following sections.

#### 3.4.7 Summary

One way of choosing an effective striation size is to match the autocorrelation function curvature at the origin

$$R_\phi''(0) = -\frac{1}{2\sigma^2} = -\frac{\sigma_\phi^2}{\sigma_\phi^2} \quad (105)$$

If this is inserted in Equation 104, the result is

$$\overline{\theta^2} = \frac{\lambda^2 \sigma_\phi^2}{4\pi^2} \frac{1}{1 - \exp(-\sigma_\phi^2)} \quad (106)$$

$$= \frac{\sigma_0^2}{1 - \exp(-\sigma_\phi^2)} \quad (107)$$

where the value for  $\sigma_0^2$  has been taken from Equation 47.

Writing  $\overline{\sigma^2}$  in this form clearly illustrates that for the general case it has the proper limiting values of  $\sigma_0^2$  for large  $\sigma_\phi^2$  and  $\sigma_\theta^2/\sigma_\phi^2$  for small  $\sigma_\phi^2$  and for the uniform striation case is correct throughout.

It is useful to think of the signal as comprising a true, undistorted signal due to the unmodified component and a noise signal due to the randomly fluctuating scattered component. In those terms, the resulting signal-to-noise ratio due to the scattering is

$$S/N = \frac{\exp(-\sigma_\phi^2)}{1 - \exp(-\sigma_\phi^2)} \quad (108)$$

### 3.5 Monopulse Response to Scattering

The important question to answer is the response of a piece of equipment to the signal produced by the scattering environment. It will be assumed that the radar pulse is sufficiently long that the signals propagated by the various scatter paths are contemporary in the signal processor. The model to be developed will be that of a phase comparison monopulse system.

A "strong" scattering case model<sup>(3)</sup> has been previously developed. The analysis was specifically applicable under conditions satisfying geometric optics. The analysis here will use the wave front integral and thin phase screen approximation that is applicable under the single, less stringent condition that the phase shift variance is large. (The results will be seen to be identical to those of the earlier, more restrictive derivation.) The analysis will then be extended to conditions of small phase shift variance.

### 3.6.1 Sum and Difference Channel Signal Formulations

Figure 2 shows the geometry of the configuration. The antenna is a phased array pointing on angle  $\alpha$  from the source. The total phase shift relative to the direct path is

$$\phi_T = -\frac{2\pi}{\lambda} \left( \frac{y^2}{2R_T} + \frac{(y-z)^2}{2r} + z \sin \alpha \right) + \phi \quad (109)$$

$$= -\frac{2\pi}{\lambda} \left( \frac{y^2}{2R} - \frac{yz}{r} + z\alpha \right) + \phi, \quad (110)$$

where a term in  $z^2/\lambda r$  has been dropped because it is small in the far zone of the antenna;  $\sin \alpha$  has been represented by  $\alpha$  (a writing simplification, not really a mathematical approximation);  $R^{-1} = R_T^{-1} + r^{-1}$  as before; and higher order terms in  $z/r$ ,  $y/r$ , and  $y/R_T$  have been dropped because scattering angles have been assumed to be small.

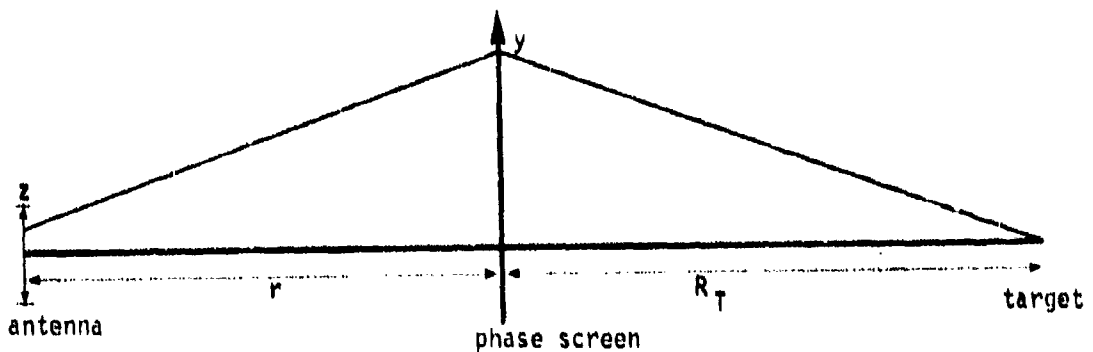


Figure 2. Antenna - scattering configuration.

For an antenna of width  $d$ , the normalized monopulse sum channel amplitude is

$$\Sigma = \int_{z=-d/2}^{d/2} \int_{-\infty}^{\infty} \phi_T dy dz \quad (111)$$

$$= \int_{-d/2}^{d/2} \int_{-\infty}^{\infty} \exp\left[-\frac{12\pi y^2}{2\lambda R} + \frac{12\pi}{\lambda} \left(\frac{y}{r} - \alpha\right) z + i\phi\right] dy dz \quad (112)$$

$$= 2 \int_0^{d/2} \int_{-\infty}^{\infty} \exp\left[-\frac{12\pi y^2}{\lambda R} + i\phi\right] \cos\left[\frac{2\pi}{\lambda} \left(\frac{y}{r} - \alpha\right) z\right] dy dz \quad (113)$$

$$= \int_{-\infty}^{\infty} \frac{\sin \frac{\pi d}{\lambda} \left(\frac{y}{r} - \alpha\right)}{\frac{\pi}{\lambda} \left(\frac{y}{r} - \alpha\right)} \exp\left[-\frac{12\pi y^2}{\lambda R} + i\phi\right] dy \quad (114)$$

To make the mathematics tractable the antenna pattern  $(\sin x/x)$  will be approximated by a gaussian. In the final application, some of the gaussian factors cancel, so that the approximation is only equivalent to fitting the antenna pattern with a gaussian locally about the region of maximum return. Using

$$\frac{\sin x}{x} \approx 1 - \frac{x^2}{6} = \exp\left(-\frac{x^2}{6}\right) \quad (115)$$

Equation 114 becomes

$$\Sigma = d \int_{-\infty}^{\infty} \exp\left\{-\frac{12\pi y^2}{\lambda R} - \frac{\pi^2 d^2}{6\lambda^2} \left(\frac{y}{r} - \alpha\right)^2 + i\phi\right\} dy \quad (116)$$

\* In actual practice, the gaussian may be a better approximation to an antenna pattern because feed tapering is used to suppress the side lobes associated with uniform illumination of a rectangular aperture.

For future writing simplicity denote

$$\begin{aligned}
 b &= \pi/\lambda R \\
 c &= \pi^2 d^2 / 6\lambda^2.
 \end{aligned}
 \tag{117}$$

The difference channel output will be

$$\Delta = \int_{z=0}^{d/2} \int_{-\infty}^{\infty} c e^{i\phi_T} dy dz - \int_{z=-d/2}^0 \int_{-\infty}^{\infty} e^{i\phi_T} dy dz
 \tag{118}$$

$$= 2i \int_{y=-\infty}^{\infty} \int_{z=0}^{d/2} \exp[-iby^2 + i\phi] \sin\left[\frac{2\pi}{\lambda} \left(\frac{y}{r} - \alpha\right) z\right] dz dy
 \tag{119}$$

$$= i \int_{-\infty}^{\infty} \left[ \frac{1 - \cos \frac{\pi}{\lambda} \left(\frac{y}{r} - \alpha\right) d}{\frac{\pi}{\lambda} \left(\frac{y}{r} - \alpha\right)} \right] \exp[-iby^2 + i\phi] dy
 \tag{120}$$

$$= \frac{i\pi d^2}{2\lambda} \int_{-\infty}^{\infty} \left(\frac{y}{r} - \alpha\right) \exp\left[-iby^2 - \frac{c}{4} \left(\frac{y}{r} - \alpha\right)^2 + i\phi\right] dy
 \tag{121}$$

where a gaussian approximation to the antenna pattern has been used once again.

### 3.5.2 Sum Channel Power

For normalization purposes, compute the undisturbed sum channel voltage and voltage variance, which is proportional to the power, for  $\phi = 0$ ,  $\alpha = 0$ .

$$\Sigma_0 = d \int_{-\infty}^{\infty} \exp[-iby^2 - cy^2/r^2] dy \quad (122)$$

$$= d \sqrt{\frac{\pi}{\frac{c}{r^2} + 1b}} \quad (123)$$

$$P_0 = |\Sigma_0|^2 = \Sigma_0 \Sigma_0^* = \frac{d^2 \pi}{\sqrt{\frac{\pi^2 d^4}{36\lambda^4 r^4} + \frac{\pi^2}{\lambda^2 R^2}}} \quad (124)$$

In the antenna far field  $d^2/\lambda r \ll 1$ ; hence Equation 124 is nearly

$$P_0 = d^2 \lambda R \quad (125)$$

Consider next the mean value of the sum channel voltage. The distribution function of the phase shift of the phase screen is

$$P(\phi) = \frac{1}{\sqrt{2\pi} \sigma_\phi} \exp(-\phi^2/2\sigma_\phi^2) \quad (126)$$

so that

$$\bar{\Sigma} = \int_{-\infty}^{\infty} \int_{-\infty}^{\infty} \frac{d}{\sqrt{2\pi} \sigma_\phi} \exp \left\{ -iby^2 - c\left(\frac{y}{r} - \alpha\right)^2 + i\phi - \phi^2/2\sigma_\phi^2 \right\} dy d\phi \quad (127)$$

This integral is the form of that of Appendix A. Because the variables are independent, integrate on  $\phi$  first. This leads to

$$\bar{\Sigma} = \frac{d \sqrt{\lambda R}}{\sqrt{T}} e^{-\frac{\sigma_{\phi}^2}{2}} e^{-\frac{\pi^2 \alpha^2 d^2}{6 \lambda^2}} \quad (128)$$

where the far zone approximation ( $c \ll lbr$ ) has been used.

Care must be exercised either in the interpretation of  $\bar{\Sigma}$  or  $\sigma_{\phi}^2$  because of antenna filtering effects. If  $\sigma_{\phi}^2$  is based upon all spatial wavelengths that might be present in the environmental structure including those comparable to the subtense of the antenna beam (i.e.,  $\phi$  varies systematically over the antenna beam), there is a portion of the signal phase variability that is constant over the beam at a particular time but varies with time. A phasor plot of the signal may just be a nearly constant amplitude vector rotating, possibly slowly, about the origin. In this case, it is the vector average of the signal which has the value given by Equation 128. Even a nonscintillating signal may have a nearly zero mean due to a slowly varying gross phase shift.

A possibly more useful approach is to include a spatial wavelength cutoff in the computation of  $\sigma_{\phi}$  such that the ensemble average of Equation 127 has some valid meaning in the context of a single measurement. The longer wavelength structure would then be accounted for by means of a mean phase shift, gross refractive angular error and focusing gain (to represent mean phase shift, mean first spatial derivative and mean second derivative). The proper way to separate the effects that are due to random variations within a beamwidth and those due to correlated variations has not been developed.

Similar, but even more stringent limitations may apply in the case of small phase perturbations or small mean scattering angle because the region of significance may be even smaller than the antenna beamwidth. It may be controlled by the mean scattering angle or a Fresnel zone.

If the one-way power gain of the antenna relative to boresight is called  $G(\alpha)$ , Equation 128 can also be written

$$\overline{\Sigma} = d \sqrt{\lambda R / T} e^{-\frac{\sigma_{\phi}^2}{2}} G(\alpha)^{1/2} \quad (129)$$

The square of the real part of  $\overline{\Sigma}$  is

$$\overline{\Sigma} \overline{\Sigma}^* = P_0 e^{-\sigma_{\phi}^2} G(\alpha) \quad (130)$$

which (by comparison with Equation 85) is the direct unmodified power attenuated by the off-axis rejection of the antenna.

Compute next the mean power received

$$\begin{aligned} \overline{P} &= \overline{\Sigma \Sigma^*} \\ &= d^2 \int_{-\infty}^{\infty} \int_{-\infty}^{\infty} \exp \left\{ i b (-y^2 + z^2) - c \left( \frac{y}{r} - \alpha \right)^2 - c \left( \frac{z}{r} - \alpha \right)^2 \right. \\ &\quad \left. + i \phi(y) - i \phi(z) \right\} dy dz \quad (131) \end{aligned}$$

Let  $z = y + \xi$

$$\bar{P} = d^2 \int_{-\infty}^{\infty} \int_{-\infty}^{\infty} \exp \left\{ i b (2y\xi + \xi^2) - 2c \left( \frac{y}{r} - \alpha \right)^2 - \frac{2c}{r} \left( \frac{y}{r} - \alpha \right) \xi \right. \\ \left. - \frac{c\xi^2}{r^2} + i(\phi(y) - \phi(y + \xi)) \right\} dy d\xi \quad (132)$$

The only factor that needs averaging over the ensemble is that involving the screen phase shifts. This was previously defined (Equation 73) as the autocorrelation function of the electric field  $R_E(\xi)$  and evaluated to be

$$R_E(\xi) = \exp \left\{ -\sigma_\phi^2 [1 - R(\xi)] \right\} \quad (133)$$

Equation 132 can then be rewritten as

$$\bar{P} = d^2 \int_{-\infty}^{\infty} \int_{-\infty}^{\infty} \exp \left\{ \xi^2 \left[ i b - \frac{c}{r^2} \right] + \xi \left[ i 2by - \frac{2c}{r} \left( \frac{y}{r} - \alpha \right) \right] \right. \\ \left. - 2c \left( \frac{y}{r} - \alpha \right)^2 - \sigma_\phi^2 [1 - R(\xi)] \right\} dy d\xi \quad (134)$$

In the limit that  $\sigma_\phi^2 \gg 1$ , the integrand is sharply peaked about  $\xi = 0$  where the term  $[1 - R(\xi)]$  is nearly zero. Consequently, the Taylor series approximation can be used for  $R(\xi)$  (see Equation 59):

$$\sigma_\phi^2 [1 - R(\xi)] = \sigma_\phi^2 \xi^2 / 2 \quad (135)$$

With this approximation, Equation 134 can be integrated first over  $\xi$  then  $y$  to produce

$$\bar{P} = \frac{P_0}{\sqrt{1 + \frac{4\pi^2 \sigma_\psi^2}{6 \theta_0^2}}} \exp \left\{ - \frac{\pi^2 \alpha^2}{3 \left( \theta_0^2 + \frac{4\pi^2}{6} \right) \sigma_\psi^2} \right\}, \quad (136)$$

where terms small in the far zone have been dropped,  $\sigma_\theta = \frac{\lambda}{2\pi} \sigma_\phi$ ,  $\sigma_\psi = R\sigma_\theta/r$  and  $\theta_0 = \lambda/d$  (the position of the first null in a rectangular antenna's side lobe pattern). This can also be written in terms of the antenna gain at angle  $\alpha$

$$\bar{P} = \frac{P_0}{\sqrt{1+u}} \exp \left( \frac{\pi^2 \alpha^2}{3 \theta_0^2} \frac{u}{1+u} \right) G(\alpha), \quad (137)$$

where

$$u = 4\pi^2 \sigma_\psi^2 / 6 \theta_0^2. \quad (138)$$

It can be shown that if  $\pi^2 \alpha^2 / 3 \theta_0^2$  is greater than 0.5, scattering may increase the signal strength over the value obtained in a non-structured environment. Basically, this means that if the target is sufficiently far from the beam pointing direction, scattering may provide a higher gain path for the energy than the direct path.

It is clear that the mean power greatly exceeds the power in the unmodified component if  $\sigma_\phi \gg 1$ . Furthermore, inspection of Equation 116 shows that the signal is effectively composed of many randomly phased components because, for the assumptions used, the  $i\phi$  term can vary over many radians within the beamwidth and Fresnel zones. As a consequence of the

central limit theorem, in this limit, the sum channel voltage will have in-phase and quadrature components that are each independently gaussianly distributed with a variance equivalent to half the received power.

For  $\sigma_\phi^2 \ll 1$ , an alternate assumption allows integration of Equation 134. The exponential factor involving the autocorrelation function can be expanded as a Taylor series in  $\sigma_\phi^2$  with the retention of only the linear term in  $\sigma_\phi^2$ . Thus,

$$e^{-\sigma_\phi^2 [1-R(\xi)]} = e^{-\sigma_\phi^2} e^{\sigma_\phi^2 R(\xi)} \quad (139)$$

$$= e^{-\sigma_\phi^2} [1 + \sigma_\phi^2 R(\xi)] \quad (140)$$

The autocorrelation function can then be approximated by a gaussian,  $\exp(-u\xi^2/2)$ , and the result inserted in Equation 134. The gaussian autocorrelation function is exact only for uniform size striations if the profile is gaussian (this can be deduced from Equation 12 and will be discussed later). However, inasmuch as it is the only physically reasonable function that renders Equation 134 integrable, we will use it in the hopes of obtaining at least a reasonable estimate of the scattering.

For these approximations,

$$\begin{aligned} \bar{P} = & d^2 c^{-\sigma_\phi^2} \iint \exp \left\{ \xi^2 \left[ 1b - \frac{c}{r^2} \right] + \xi \left[ 12by - \frac{2c}{r} \left( \frac{y}{r} - \alpha \right) \right] - 2c \left( \frac{y}{r} - \alpha \right)^2 \right\} \\ & \times \left\{ 1 + \sigma_\phi^2 \exp[-u\xi^2/2] \right\} dy d\xi \quad (141) \end{aligned}$$

This is of the same form as previous integrals. If we make the far zone approximation ( $c^2 \ll b^2 r^4$ ), match the curvature of the autocorrelation function of the phase at the origin ( $a = \sigma_\phi^2 / \sigma_\phi^2$ ), and, in the limit of small  $\sigma_\phi^2$ , approximate  $\sigma_\phi^2$  by  $\exp(\sigma_\phi^2) - 1$ , we obtain for the integral

$$\bar{P} = P_0 \left\{ e^{-\sigma_\phi^2} \exp\left[-\frac{\pi^2 d^2 \alpha^2}{3\lambda^2}\right] + \frac{1 - e^{-\sigma_\phi^2}}{\sqrt{1 + \frac{d^2 R^2 \sigma_\phi^2}{6 r^2 \sigma_\phi^2}}} \exp\left[-\frac{\pi^2 d^2 \alpha^2}{3\lambda^2 \left(1 + \frac{d^2 R^2 \sigma_\phi^2}{6 r^2 \sigma_\phi^2}\right)}\right] \right\} \quad (142)$$

This can also be written in terms of the antenna beamwidth  $\theta_0$  and mean apparent scattering variance  $\sigma_\psi^2$ .

$$\bar{P} = P_0 \left\{ e^{-\sigma_\phi^2} G(\alpha) + \frac{1 - e^{-\sigma_\phi^2}}{\sqrt{1 + \frac{2\pi^2 \sigma_\psi^2}{3\theta_0^2 \sigma_\phi^2}}} \exp\left[-\frac{\pi^2 \alpha^2}{3\left(\theta_0^2 + \frac{2\pi^2 \sigma_\psi^2}{3\sigma_\phi^2}\right)}\right] \right\} \quad (143)$$

By reference to Equation 130, it can be seen that the first term is exactly the power associated with the unmodified component, and the second term must be that produced by the random noisy component. If the derived value of the mean scattering variance is obtained from Equation 107

$$\bar{\psi}^2 = \left(\frac{R}{r}\right)^2 \bar{\theta}^2 \quad (144)$$

$$= \frac{\sigma_\psi^2}{1 - \exp(-\sigma_\phi^2)} \quad (145)$$

and the asymptotic forms for large and small  $\sigma_\phi^2$  are used in the expressions for strong scattering, Equation 136, and weak scattering, Equation 143, the result in both cases is

$$\bar{P} = P_0 \left\{ \sigma^{-\sigma_\phi^2} G(\alpha) + \frac{1 - e^{-\sigma_\phi^2}}{\sqrt{1 + \frac{2\pi^2 \psi^2}{3 \theta_0^2}}} \exp \left[ - \frac{\pi^2 \alpha^2}{3 \left( \theta_0^2 + \frac{2\pi^2 \psi^2}{3} \right)} \right] \right\} \quad (146)$$

Thus, we have a single expression valid for both strong and weak scattering.

### 3.5.3 Sum Channel Amplitude Distribution

For strong scattering, it was shown that the sum channel signal was composed of two independent gaussian variates in quadrature. How is it for weak scattering? Expand the basic sum channel voltage given in Equation 116 for small phase shifts.

$$\Sigma = d \int_{-\infty}^{\infty} \exp \left\{ -lby^2 - c \left( \frac{y}{r} - \alpha \right)^2 \right\} [1 + i\phi + \dots] dy \quad (147)$$

$$= \Sigma_0 + d \int_{-\infty}^{\infty} \exp \left\{ -lby^2 - c \left( \frac{y}{r} - \alpha \right)^2 \right\} i\phi dy \quad (148)$$

This shows the sum signal is nearly the undistorted signal plus a weighted integral of the phase shift. The integral is the limit of a sum. Consequently, the integral over the weighted gaussian variate  $\phi$  will be a gaussian variate. Consider the integral as a summation. There will be regions of  $y$  in which the phase is relatively constant. Call the width of such a region  $\xi_1$  and take it to be the distance for the autocorrelation function to drop to 0.5,

$$\xi_1 \approx \frac{\sigma_\phi}{\sigma_\phi} . \quad (149)$$

The character of the integral of Equation 148 is that there is general attenuation near  $y=0$  of  $\exp(-\alpha^2)$ , which is the antenna response in the target-source direction, and a continuously changing phase. The regions of coherent plasma phase shift will be coherent in the integration only if the spatial phase change across the region  $\xi_1$  is small. Outside that region, the phase becomes randomized and does not add coherently. The phase shift gradient due to physical path length is

$$\frac{d\phi_s}{dy} = \frac{2\pi y}{\lambda R} \quad (150)$$

For estimation purposes, require that

$$\frac{d\phi_s}{dy} \xi_1 < \frac{\pi}{2} . \quad (151)$$

This establishes a maximum region of the phase screen  $y_m$  outside of which the spatial variation of phase is so rapid as to prevent coherent phase addition. Thus,

$$y_m = \frac{\lambda R}{4\xi_1} . \quad (152)$$

If the structure dimensions are small compared to the first Fresnel zone, the total spatially induced phase shifts involved in  $y_m$  are large compared to  $2\pi$ . The contribution of the phase shift should be nearly random so long as the total phase shift in  $y_m$  is large compared to  $2\pi$ . Across each element  $\xi_1$ , the contribution to the integral of Equation 148 has a variance

$$\Delta P \approx d^2 \xi_1^2 G(\alpha) \sigma_\phi^2 . \quad (153)$$

Of this, because the phase shift associated with the exponential factor in Equation 148 spans a large variation, on the average, half the contribution will be in phase with the unmodified component and half in quadrature.

The number of such independent samples will be

$$n = 2y_m / \epsilon_1 \quad (154)$$

The variance of the sum of  $n$  samples is  $n$  times the variance of the single sample. Thus, the in-phase component of scattered power is

$$P_X = \frac{1}{4} d^2 \lambda R \sigma_\phi^2 G(\alpha) \quad (155)$$

$$= \frac{1}{4} P_0 \sigma_\phi^2 G(\alpha) \quad (156)$$

The result of Equation 156 is comparable to the scattered component in Equation 146. It differs in that the sum of the in-phase and an equal magnitude quadrature power is half of that obtained in the detail calculation, which is reasonably close considering the ad hoc assumptions used in the crude derivation. It also differs by the neglect of  $\frac{2\pi^2}{5} \psi^2$  compared to  $0\frac{1}{2}$ , but this is valid for  $\sigma_\phi \ll 1$  if the plasma structural dimensions are small compared to the first Fresnel zone.

The information added by this quantitatively more crude analysis is that the scattered component consists of independent in-phase and quadrature gaussian components. This of course leads to Rician statistics for the power.

In addition to the evenly divided components there is an additional contribution of a random component in quadrature to the direct signal that is due to the large extent of the first Fresnel zone. However, it can be

shown to be smaller by the ratio of the plasma structural dimension to the first Fresnel zone size. This has been referred to as Fresnel filtering and may be significant for some combinations of  $\sigma_\phi$  and spatial autocorrelation function.

### 3.5.4 Difference Channel Power

Consider now the difference channel, for which the signal voltage is given by Equation 121. If the phase perturbation is zero, the undisturbed reference signal is obtained. Thus,

$$\Delta_0 \approx \frac{1}{2\lambda} \int_{-\infty}^{\infty} \left( \frac{y}{r} - \alpha \right) \exp \left\{ y^2 \left( -1b - \frac{c}{4r^2} \right) + \frac{c\alpha}{r} y - \frac{c}{4} \alpha^2 \right\} dy \quad (157)$$

In the far zone of the antenna, this is

$$\Delta_0 \approx -d/\sqrt{\lambda r} \left( \frac{\pi\alpha}{2\theta_0} \right) \exp \left( -\frac{\pi^2 \alpha^2}{24\theta_0^2} \right) . \quad (158)$$

It can be seen by reference to Equation 123 that the difference channel is in quadrature to the sum channel. Furthermore, the exponential term is just the antenna gain of each half the antenna used to form the difference beam, or specifically  $\sqrt{G(\alpha/2)}$ . The other term in the parenthesis is just the small angle approximation to the normal difference channel function  $\sin(p\alpha)$  where  $p$  is  $\pi d/2\lambda$ . Thus,

$$\Delta_0 \Delta_0^* = P_0 \sin^2(p\alpha) G(\alpha/2) . \quad (159)$$

In the presence of phase fluctuations, the variance of the difference channel voltage will differ from that given by Equation 159. It can be computed in a manner similar to that of the sum channel:

$$\Delta\Delta^* = \frac{d^4}{\lambda^2} \iint \left( \frac{y}{r} - \alpha \right) \left( \frac{z}{r} - \alpha \right) \frac{\pi^2}{4} \exp \left\{ -ib(y^2 - z^2) - \frac{c}{4} \left[ \left( \frac{y}{r} - \alpha \right)^2 + \left( \frac{z}{r} - \alpha \right)^2 \right] + 1[\phi(y) - \phi(z)] \right\} dy dz. \quad (160)$$

If the substitution  $z = y + \xi$  is used and the phase difference averaged over the ensemble, the result is

$$\overline{\Delta\Delta^*} = \frac{d^4}{\lambda^2} \iint \frac{\pi^2 \eta}{4} \left( \eta + \frac{\xi}{r} \right) \exp \left\{ \left( 1b - \frac{c}{4r^2} \right) \xi^2 + \left( 12by - \frac{c\eta}{2r} \right) \xi - \frac{c}{2} \eta^2 - \sigma_\phi^2 [1 - R(\xi)] \right\} dy d\xi \quad (161)$$

where  $\eta = \frac{y}{r} - \alpha$ .

For the case of large phase perturbations, the term involving the autocorrelation function can be approximated by

$$\sigma_\phi^2 [1 - R(\xi)] = \begin{cases} \frac{1}{2} \sigma_\phi^2, & \xi^2 < \frac{2 \sigma_\phi^2}{\sigma_\phi^2} \\ \sigma_\phi^2, & \xi^2 > \frac{2 \sigma_\phi^2}{\sigma_\phi^2} \end{cases} \quad (162)$$

As was discussed for the sum channel power, the integral on  $\xi$  in Equation 161 can be broken at  $\xi^2 = 2\sigma_\phi^2/\sigma_\phi^2$ . The integral for large  $\xi$  just gives the unmodified component times an attenuation factor  $\sigma^{-\sigma_\phi^2}$  plus an attenuation of the scattered component that averages  $1 - e^{-\sigma_\phi^2}$ .

Let us concentrate on the portion of the integral near the origin. As a matter of fact, the term  $\exp(-\sigma_\phi^2 \xi^2/2)$  becomes so small outside the interval of concern that the limits on the integral can be extended to infinity with little introduction of error. Thus, the mean scattered component is

$$\overline{\Delta\Delta_s^*} = \frac{d^4}{\lambda^2} \iint_{-\infty}^{\infty} \frac{\pi^2 \eta}{4} \left( \eta + \frac{\xi}{r} \right) \exp \left\{ -\xi^2 \left[ \frac{c}{4r^2} + \frac{\sigma_{\phi'}^2}{2} - 1b \right] + \xi \left[ 1.2by - \frac{c\eta}{2r} \right] - \frac{c\eta^2}{2} \right\} dy d\xi. \quad (163)$$

Straightforward application of Appendix A to first  $\xi$  then  $y$  yields

$$\overline{\Delta\Delta_s^*} = \frac{P_0 \left\{ \left( \frac{\pi\alpha}{2\theta_0} \right)^2 + \frac{3u}{8} \left( 1 + \frac{u}{4} \right) \right\}}{\left( 1 + \frac{u}{4} \right)^{3/2}} \exp \left\{ - \frac{\pi^2 \alpha^2}{12\theta_0^2 \left( 1 + \frac{u}{4} \right)} \right\}. \quad (164)$$

The first term in the curly brackets replaces what was the difference signal  $\sin^2(\rho\alpha)$  and comprises a component that is a function of the direction off the monopulse null and a component dependent only on the scattering, which makes the object have the appearance of moving around off-boresight.

It is interesting to rewrite Equation 164 in terms of an effective angle  $\alpha' = \alpha/\sqrt{1+u/4}$ . As will be seen the effect of the scattering can be interpreted as moving the apparent position of the source closer to boresight by the factor  $1/\sqrt{1+u/4}$ . Equation 164 becomes

$$\overline{\Delta\Delta_s^*} = \frac{P_0}{\left( 1 + \frac{u}{4} \right)^{3/2}} G(\alpha'/2) \sin^2(\rho\alpha') \left[ 1 + \frac{\sigma_{\psi}^2}{\alpha'^2} \right]. \quad (165)$$

This can be interpreted in terms of a power loss due to the scattering and the reduction in effective boresight angle, and shows that the relative magnitude of the non-boresight dependent term is just the ratio of the variance of the phase screen scattering, as viewed from the radar, to the square of the apparent off-boresight angle.

In summary, for  $\sigma_\phi^2 \gg 1$ , the difference channel signal comprises an attenuated unmodified component  $\Delta_0 \exp(-\sigma_\phi^2/2)$  and a scattered random component that can be argued, in a manner similar to that for the sum channel, to have independent random in-phase and quadrature components with variance  $[1 - \exp(-\sigma_\phi^2)] \overline{\Delta\Delta^*}/2$ .

Consider now the weak perturbation case. As for the case of the sum channel, the random phase effects will be approximated by taking

$$\exp\{-\sigma_\phi^2[1-R(\xi)]\} = \exp(-\sigma_\phi^2) + [1 - \exp(-\sigma_\phi^2)]R(\xi). \quad (166)$$

With the use of this approximation, Equation 161 becomes the sum of two integrals. The first is exactly  $\exp(-\sigma_\phi^2) \Lambda_0 \Delta_0^*$ .

If the autocorrelation function is once more approximated by a gaussian,  $R(\xi) = \exp(-\sigma_\phi^2 \xi^2 / 2\sigma_\phi^2)$ , one sees that the second integral is identical in form to that integrated for strong scattering except that wherever  $\sigma_\phi^2$ , appeared originally,  $\sigma_\phi^2 / \sigma_\psi^2$  now appears. As was discussed earlier, this is equivalent to replacing  $\sigma_\phi^2$  by  $\overline{\psi^2}$  where

$$\overline{\psi^2} = \frac{\sigma_\psi^2}{1 - \exp(-\sigma_\phi^2)} \quad (167)$$

With this modification, the same equations apply in both limits  $\sigma_\phi^2 \ll 1$  and  $\sigma_\phi^2 \gg 1$ .

### 3.5.5 Summary of Monopulse System Output

In summary, this gives a unified means of computing the sum and difference channel signals. The equations are explicitly valid for large and small values of  $\sigma_\phi$  and it is assumed that they can't be too far off for  $\sigma_\phi \approx 1$ . The environment is defined in terms of  $\sigma_\phi^2$  and either  $\sigma_\phi^2$ ,

or  $\sigma_\psi^2$  which are related by  $\sigma_\psi = R\lambda\sigma_\phi/2\pi r$ . Means for computing these parameters from an environmental description were given in an earlier section and specific examples follow in the next section.

The radar system is characterized by antenna beamwidths  $\theta_0$  ( $=\lambda/d$ ), the first null in a rectangular aperture's pattern, and  $\theta_b$ , the -3 dB power beamwidth which, for a rectangular aperture, is related to  $\theta_0$  by  $\theta_b = 2.8\theta_0/\pi$ . The sum beam relative power gain an angle  $\alpha$  from beam center is  $G(\alpha)$ . The on-axis, undisturbed sum beam signal power is  $P_0$ . The undisturbed difference beam power is  $P_0 G(\alpha/2) \sin^2(p\alpha)$  where  $p = \pi d/2\lambda$ .

A parameter characterizing the relative importance of scattering and antenna rejection is

$$u = \frac{2\pi^2 \overline{\psi^2}}{30\theta_0^2} = \frac{5.23 \overline{\psi^2}}{\theta_b^2} \quad (168)$$

Using these basic inputs, the sum channel signal comprises an unmodified component of power

$$P_u = P_0 \exp(-\sigma_\phi^2) G(\alpha) \quad (169)$$

and two orthogonal, random, independent components, each gaussianly distributed of variance

$$P_s = \frac{P_0}{2} [1 - \exp(-\sigma_\phi^2)] \exp\left[\frac{2.6\alpha^2}{\theta_b^2} \frac{u}{1+u}\right] \frac{G(\alpha)}{\sqrt{1+u}} \quad (170)$$

The difference channel comprises an unmodified component in quadrature to the unmodified sum channel signal and a scattered signal. The unmodified component has a power associated with it of

$$\Delta_0 \Delta_0^* = P_0 \exp(-\sigma_\phi^2) G(\alpha/2) \sin^2(px). \quad (171)$$

The scattered component comprises phase orthogonal, independent random gaussian components with variance

$$\overline{\Delta \Delta_{x,y}^*} = \frac{P_0}{2 \left(1 + \frac{u}{4}\right)^{3/2}} G(\alpha/2 \sqrt{1+u/4}) \left\{ \frac{2\alpha^2}{b} + \frac{3u}{8} \left(1 + \frac{u}{4}\right) \right\}. \quad (172)$$

It should be pointed out that on the current effort possible correlation between the sum and difference channel signals has not been analyzed and the difference channel analysis has assumed that the target is displaced along one of the axes of the monopulse system and that the striation axes are aligned with the other. Analysis to overcome these shortcomings is straightforward but there was insufficient time to fully explore all aspects of the processor.

#### 4. SCATTERING BY VARIOUS PLASMA STRUCTURES

This section will investigate the relative scattering produced by different size distributions of striations to determine the sensitivity of scattering calculations to details of the distribution. The problem is that the distribution is not well established, so if there were a great sensitivity to plasma parameters, there could be little reliance in the quantification of the scattering.

##### 4.1 Model Descriptions

Four models of the distribution of striation sizes will be considered as illustrative distributions. The particular models were chosen for simplicity or prior use in the literature. The models are single, uniform size, a modification of Chesnut's distribution, and power law distributions with either fixed or size-dependent axial electron content.

#### 4.1.1 Model 1

In this distribution all striations have the same characteristic radius and peak electron concentration. The probability distribution function of the radii is a delta function,  $\delta(\sigma - \sigma_0)$ . This is an idealized model that is easy to visualize and to work with. Because it is so simple, the results of analysis of the scattering properties of other distributions will be expressed in terms of an effective striation size. That is, the characteristic dimension of uniform striations needed to produce the same scattering will be determined.

#### 4.1.2 Model 2

This distribution was inferred by Walter Chesnut from an analysis of photographic data. The probability density function is

$$P(\sigma) = \frac{n}{\sigma_0} \left( \frac{\sigma_0}{\sigma} \right)^n \exp\left(-\frac{\sigma_0^2}{\sigma^2}\right). \quad (173)$$

Reasonable distributions (i.e., finite phase shift) imply that  $n$  exceeds 4. The normalization factor  $n$  is

$$n = \frac{2^{n-2} \left( \frac{n-1}{2} \right)!}{\sqrt{\pi} (n-3)!}, \quad n \text{ even} \quad (174)$$

$$n = \frac{2}{\left( \frac{n-3}{2} \right)!}, \quad n \text{ odd}, \quad (175)$$

The specific power favored by Chesnut was  $n=6$  so that  $n$  was  $8/3\sqrt{\pi}$ .

A plot of this function for  $n=5, 6, 7$  and  $8$  is shown in Figure 3.

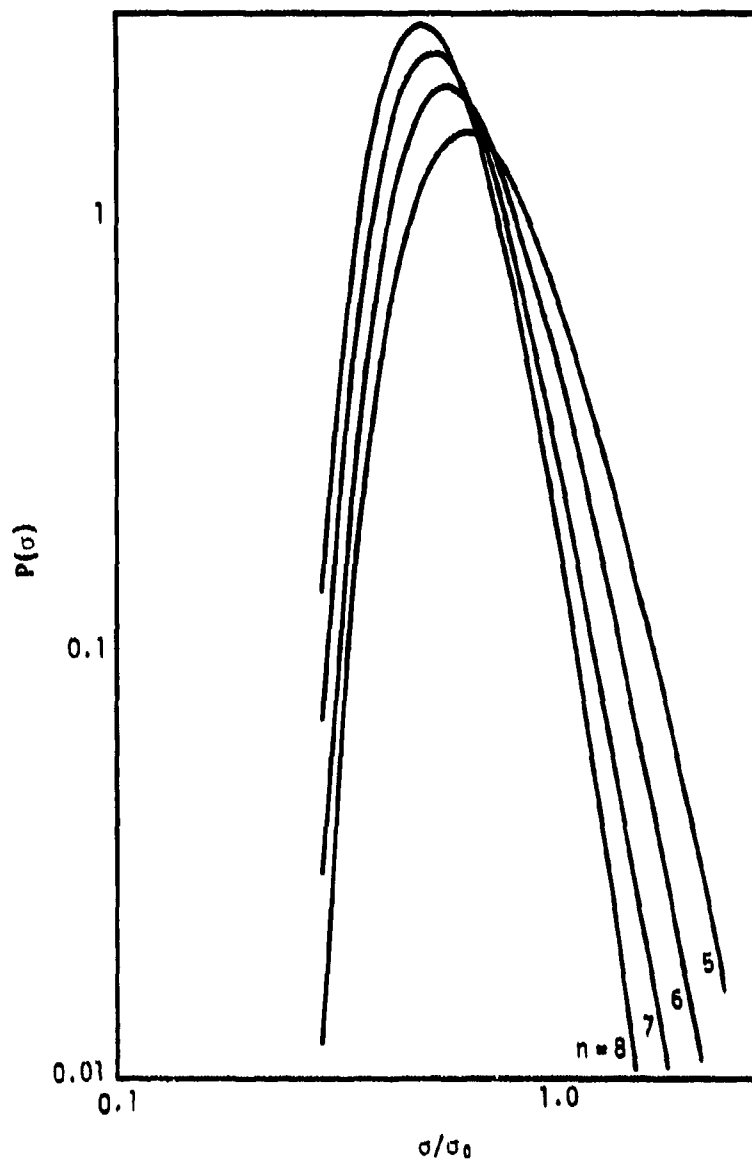


Figure 3. Probability density function for Model 2.

To relate this function to the plasma instability analysis, which yields a minimum cutoff wavelength, it is necessary to develop a definition of the characteristic striation size  $\sigma_0$ . If the cutoff size is taken to be that having a tenth the probability density at the peak of the spectrum,

$$\sigma_0 = 1.86 \sigma_c n^{1/4} \quad (176)$$

is a reasonable fit for the data of Figure 3.

As was pointed out earlier, this spectrum of radii applies specifically to fireball regions, some of the observed spatial power spectra were best matched with the sum of two distributions of the form of Equation 173, and the analysis was not very precise about the exact value of the exponent of  $\sigma_0/\sigma$ —a value of 6 seemed to fit the data as well as any. However, it is a convenient integrable form that fits the data reasonably well. Also, because the phase shift approaches a gaussian random sequence, the variances of phase shift and of derivatives of phase shift for a distribution that is the sum of several components are just the sum of the variances for each of the several components.

Another way of viewing this distribution is that it is a power law distribution with the short spatial wavelength end cut off by the exponential rather than by an abrupt limit. As such, it is probably more realistic than the pure power law distribution. The continuous function has the advantage of allowing the limits on integrals determining plasma scattering parameters to be  $\sigma = 0$  or  $\infty$ .

The axial electron concentration is assumed to be constant, independent of striation size.

#### 4.1.3 Model 3

This is a power law distribution with a normalized distribution function of

$$P(\sigma) = \frac{(s-1)}{\frac{1}{\sigma_1^{s-1}} - \frac{1}{\sigma_2^{s-1}}} \frac{1}{\sigma^s} \quad (177)$$

for  $\sigma_1 < \sigma < \sigma_2$  and zero outside those limits. This reflects the situation that below a minimum cutoff size, plasma perturbations are stable and will not grow and that structures larger than radar beam dimensions or plasma gradient distances have either no influence on the scattering problem or no meaning in terms of the plasma description used here.

There is little reason for a particular choice of power. Except for the arbitrary cutoff for large structures, this distribution would also produce infinite phase shift variance for  $s \leq 4$ .

The axial electron content is taken to be uniform.

#### 4.1.4 Model 4

This model has the same distribution function as Model 3, but the axial electron concentration is taken proportional to the striation size.

$$n_0 = n_r \sigma . \quad (178)$$

This is based upon an intuitive feeling that any growing perturbations should pinch off and stop growing once the perturbation amplitude becomes a reasonable fraction of a structural wavelength.

This was the model used in the initial HARC analysis. If all possible perturbation models are allowed in a cylindrically posed problem and modes are allowed to decorrelate in a wavelength, a value of four is deduced for  $s$ .

#### 4.2 Plasma Parameters

It will be assumed that in reasonably homogeneous regions the local electron concentration variance  $\sigma_n^2$  and a cutoff wavelength are available from either plasma analysis or experimental data. These will be used to compute the variance of phase shift and phase shift transverse gradient which can then be integrated along sight paths.

The result can be expressed in terms of an effective uniform distribution striation size. The pertinent equations are repeated here from previous sections:

$$\sigma_c^2 = \lambda_c^2/20 ;$$

Equation (27)

$$\sigma_n^2 = \pi m \int_0^\infty n_0^2 \sigma^2 P(\sigma) d\sigma = \pi m \overline{n_0^2 \sigma^2}; \quad (179)$$

Equation (30)

$$\sigma_\phi^2 = \frac{2\pi^{7/2} mL}{\lambda^2 n_c^2 \sin \alpha} \int_0^\infty n_0^2 \sigma^3 P(\sigma) d\sigma = \frac{2\pi^{7/2} mL}{\lambda^2 n_c^2 \sin \alpha} \overline{n_0^2 \sigma^3}; \quad (180)$$

and a combination of Equation 47 and 48

$$\sigma_{\phi'}^2 = \frac{\pi^{7/2} mL}{\lambda^2 n_c^2 \sin \alpha} \int_0^\infty n_0^2 \sigma P(\sigma) d\sigma = \frac{\pi^{7/2} mL}{\lambda^2 n_c^2 \sin \alpha} \overline{n_0^2 \sigma}. \quad (181)$$

The form to be ultimately used combines these to give

$$\sigma_{\phi'}^2 = \frac{\pi^{5/2} L}{\lambda^2 \sigma_e \sin \alpha} \frac{\sigma_n^2}{n_c^2} \quad (182)$$

where

$$\sigma_e = \frac{n_0^2 \sigma^2}{n_0^2 \sigma} \quad (183)$$

and

$$\sigma_{\phi}^2 = 2\sigma_f^2 \sigma_{\phi'}^2 \quad (184)$$

where

$$\sigma_f^2 = \frac{n_0^2 \sigma^3}{n_0^2 \sigma} \quad (185)$$

#### 4.2.1 Model 1

If Equations 183 and 185 are evaluated, it is apparent the striation size of the uniform striations is identically the same as  $\sigma_e$  and  $\sigma_f$ . This is, of course, the reason for having labelled the uniform size  $\sigma_e$ .

Two interesting points are developed when the scattering parameters are expressed this way. The concentration of striations and the axial electron content no longer appear explicitly in Equation 182 or 184 and the ratio of the variance of phase and phase gradient is simply related to the striation dimension. Equation 182 also implies that the variance of the scattering angle is

$$\sigma_{\theta}^2 = \frac{\sqrt{\pi} L}{\sigma_e \sin \alpha} \left( \frac{\sigma_n}{2n_c} \right)^2 \quad (186)$$

#### 4.2.2 Model 2

The effective striation size is

$$\sigma_e = \frac{\int_0^{\infty} \sigma^2 \left(\frac{\sigma_0}{\sigma}\right)^n \exp\left[-\left(\frac{\sigma_0}{\sigma}\right)^2\right] d\sigma}{\int_0^{\infty} \sigma \left(\frac{\sigma_0}{\sigma}\right)^n \exp\left[-\left(\frac{\sigma_0}{\sigma}\right)^2\right] d\sigma} \quad (187)$$

$$= \sigma_0 \frac{\int_0^{\infty} x^{n-4} \exp(-x^2) dx}{\int_0^{\infty} x^{n-3} \exp(-x^2) dx} \quad (188)$$

where  $x = \sigma_0/\sigma$ . For  $n$  even,

$$\sigma_e = 1.86 \sigma_0 n^{1/4} \sqrt{\pi} \frac{\Gamma(n-4)}{2^{n-5} \Gamma\left(\frac{n-4}{2}\right) \Gamma\left(\frac{n-2}{2}\right)} \quad (189)$$

or, for  $n$  odd,

$$\sigma_e = 1.86 \sigma_0 n^{1/4} \frac{2}{\sqrt{\pi}} \frac{2^{n-5} \left(\Gamma\left(\frac{n-3}{2}\right)\right)^2}{\Gamma(n-3)} \quad (190)$$

These are shown in Figure 4 for values of  $n$  from 4 to 9. Similarly,

$$\sigma_f^2 = 1.86^2 \sigma_c^2 n^{1/2} \frac{\int_0^{\infty} x^{n-5} \exp(-x^2) dx}{\int_0^{\infty} x^{n-3} \exp(-x^2) dx} \quad (191)$$

or

$$\sigma_f = 1.86 n^{1/4} \sqrt{\frac{2}{n-4}} \sigma_c \quad (192)$$

Values of  $\sigma_f$  are also shown in Figure 4.

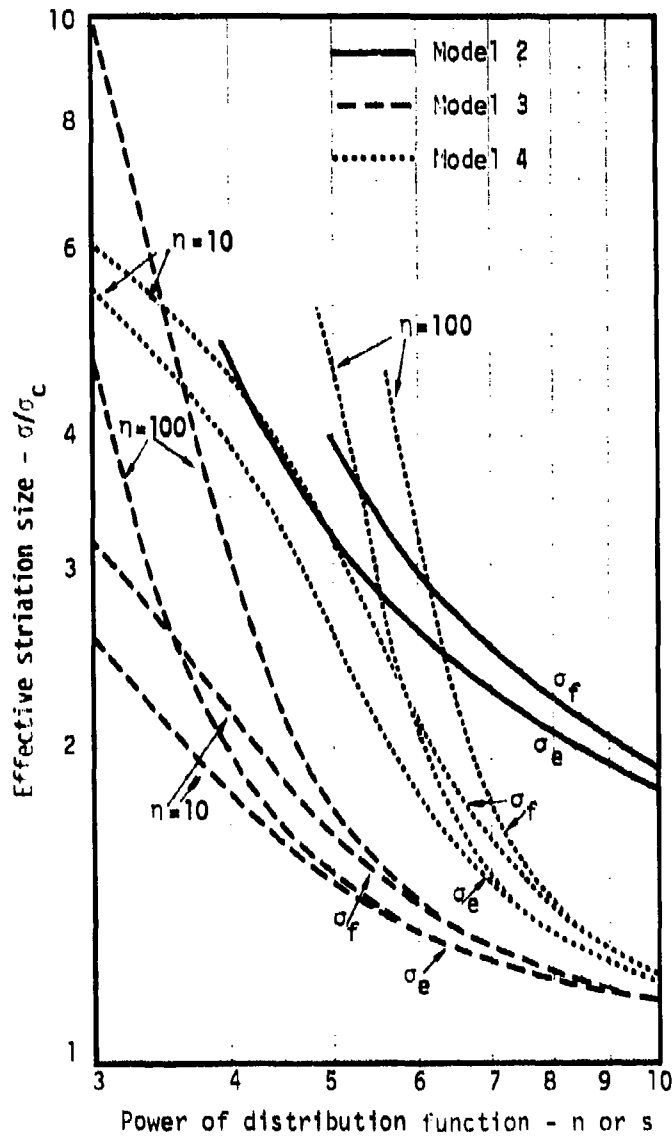


Figure 4. Effective striation sizes for the various scattering models.

#### 4.2.3 Model 3

The integrals for Model 3 are simple and yield

$$\sigma_e^2 = \frac{s-2}{s-3} \frac{1-\eta}{1-\eta} \frac{s-3}{s-2} \sigma_1^2, \quad (193)$$

and

$$\sigma_f^2 = \frac{s-2}{s-4} \frac{1-\eta}{1-\eta} \frac{s-4}{s-2} \sigma_1^2, \quad (194)$$

where  $\eta = \sigma_1/\sigma_2$ —the ratio of the lower and upper cut-off striation sizes. For distributions with  $s$  equal to 2, 3 or 4, the following limit can be used in these expressions

$$\lim_{s \rightarrow 0} \frac{1-\eta}{s} = -\ln \eta, \quad (195)$$

#### 4.2.4 Model 4

For Model 4 the effective sizes are

$$\sigma_e^2 = \frac{4-s}{5-s} \frac{1-\eta}{1-\eta} \frac{s-5}{s-4} \sigma_1^2, \quad (196)$$

and

$$\sigma_f^2 = \frac{4-s}{6-s} \frac{1-\eta}{1-\eta} \frac{s-6}{s-4} \sigma_1^2, \quad (197)$$

These are also plotted in Figure 4.

### 4.3 Comparison of Model Results

Perusal of the data in Figure 4 shows some not too surprising trends. The larger striations are emphasized (with resulting larger effective size) by lower inverse powers, by having larger axial electron content (Model 4) and by the model that rolls off more slowly at the short

wave cutoff. However, it is also noticeable that a lot of the effective striation sizes lie between 1.5 and 4 times the cutoff size. Consequently, if an effective striation size is taken to be

$$\sigma_e = \sigma_f = 2.5 \sigma_c \quad (198)$$

reasonable results are anticipated. This value is recommended because it is near that derived for the one experimental distribution. Also, the magnetic field should continue to break up the larger striations so that low powers in the distribution function shouldn't persist. Furthermore, the sharp cutoff that leads to small values of  $\sigma_e$  seems physically unrealistic. It would seem surprising if the proper effective size differed from  $2.5 \sigma_c$  by a factor of 2 and it most likely lies within a factor of 1.5.

Certainly with our current state of knowledge, there is no reason for assigning different values to  $\sigma_e$  and  $\sigma_f$ .

It should be remembered that  $\sigma_{\phi_1}^2$  and  $\sigma_{\theta}^2$  vary inversely with  $\sigma_e$ . Consequently, the scattering uncertainty introduced by the striation uncertainty is reduced by a square root process.

The phase variance  $\sigma_{\phi}^2$  varies as the product  $2\sigma_f^2 \sigma_{\phi_1}^2$ . Consequently, if the effective striation size were actually smaller than used here,  $\sigma_{\phi_1}$  would be greater and  $\sigma_{\phi}$  would be smaller, both by about the fractional error in  $\sigma_e$ .

## 5. SUMMARY AND UTILIZATION OF FORMULATIONS

It will be assumed here that in a series of regions of length  $L_1$  the cutoff plasma wavelength  $\lambda_c$  and electron concentration variance are determined from some environmental description. If other parameters such as axial electron concentration and striation size parameter are given, the formulations of Section 3.2 can be used to compute  $\sigma_n^c$ . Chesnut (and TEMPO following his work) used a profile defined as  $n_0 \exp(-r^2/\sigma_u^2)$ . If the factors accounting for the difference in profile definition, the relationship of cutoff size to characteristic size and cutoff wavelength to cutoff size are combined, the cutoff wavelength should be taken to be 1.2 times his size spectrum characteristic parameter.

### 5.1 Local Effective Striation Size

The local effective striation size can be taken to be

$$\sigma_c = \sigma_f = 0.56 \lambda_c. \quad (199)$$

The precision of this relationship should be 20 to 50 percent as estimated by comparing the results for the several distributions analyzed. The effective size is defined as the size of uniform striations in an environment having the same electron content variance needed to produce the same scattering. The same effective size can be used for relating electron content variance and scattering angle variance (or its equivalent phase derivative variance) and for relating phase variance and phase derivative variance.

### 5.2 Local Scattering Angle

Several directly related parameters have been used that define the basic angular scattering or variance of transverse derivative of phase. These are the environmental, plane wave scattering angle variance:

$$\sigma_{\theta}^2 = \frac{\sqrt{\pi} L}{\sigma_e \sin \alpha} \left( \frac{\sigma_n}{2n_c} \right)^2 ; \quad (200)$$

variance of transverse derivative of phase:

$$\sigma_{\phi'}^2 = \frac{4\pi^2}{\lambda^2} \sigma_{\theta}^2 ; \quad (201)$$

and variance of scattering as viewed by radar:

$$\sigma_{\psi}^2 = \left( \frac{R}{r} \right)^2 \sigma_{\theta}^2 . \quad (202)$$

The last of these variances indicates the proper way for weighting the scattering as a function of distance from the radar.

### 5.3 Local Phase Variance

The local phase variance is determined from the phase gradient by

$$\sigma_{\phi}^2 = 2 \sigma_f^2 \sigma_{\phi'}^2 . \quad (203)$$

### 5.4 Integrated Scattering Angle

Inasmuch as any of the local scattering angle parameters have an integrated value that is a gaussian variate, the variance of the sum is the sum of the variances of the individual contributions. Thus,

$$\sigma_{\psi}^2 = \sum_1 \left( \frac{R}{r} \right)_1^2 \sigma_{\theta_1}^2 \quad (204)$$

and

$$\sigma_{\phi'}^2 = \frac{4\pi^2}{\lambda^2} \sum_1 \sigma_{\theta_1}^2 . \quad (205)$$

## 5.5 Integrated Phase Variance and Mean Striation Size

The integrated phase also becomes a gaussian variate and the variance of integrated phase will be

$$\sigma_{\phi}^2 = \sum_1 \sigma_{\phi_1}^2 = 2 \sum_1 \sigma_{f_1}^2 \sigma_{\phi_1}^2 . \quad (206)$$

One would like to be able to obtain the integrated phase variance from the integrated derivative variance by use of a mean effective size. Thus,

$$\sum_1 \sigma_{\phi_1}^2 = 2 \overline{\sigma_f^2} \sum_1 \sigma_{\phi_1}^2 . \quad (207)$$

Comparison of Equations 206 and 207 show that this can be done if the mean effective size is formed as

$$\overline{\sigma_f^2} = \sum_1 \sigma_{f_1}^2 \sigma_{\phi_1}^2 / \sum_1 \sigma_{\phi_1}^2 . \quad (208)$$

(Because they are related by a constant,  $\sigma_{\theta}^2$  could have been used instead of  $\sigma_{\phi}^2$ , in Equation 208.) If the mean effective striation size is determined in this manner, for the total scattering layer

$$\sigma_{\phi}^2 = 2 \overline{\sigma_f^2} \sigma_{\phi}^2 . \quad (209)$$

## 5.6 Angular Scattering of Power

In the limit of small total phase perturbation ( $\sigma_{\phi}^2 < 1$ ), there is little power in the scattered signal and its angular distribution is spread by diffraction. The rms scattering angle is

$$\overline{\psi^2} = \sigma_{\phi}^2 / [1 - \exp(-\sigma_{\phi}^2)] , \quad (210)$$

which is that expected for diffraction from a structure the size of a correlation length.

In the limit of strong scattering ( $\sigma_\phi^2 \gg 1$ ) or a uniform striation weakly scattering plasma, the power is gaussianly distributed with a variance given by Equation 210. In the strong scattering multipath case, the number density of paths is gaussianly distributed with an amplitude distribution that is independent of the distance of the ray from the direct line of sight. For weak scattering the angular power spectrum may not be gaussian but its variance is still reasonably approximated by Equation 210 and usually the spectral differences are only significant if the scattering is insignificant.

### 5.7 Received Power Statistics

If the signal that propagates through the scattering medium is received by an antenna, the received power (or sum channel in a monopulse receiver) comprises an attenuated but unmodified component and both in-phase and quadrature random components. If the antenna has a sum channel one-way power gain  $G(\alpha)$  an angle  $\alpha$  from the beam center, a 3-dB, full width, one-way power beamwidth of  $\theta_b$ , and the source of the received energy is an angle  $\alpha$  from the beam center, the unmodified component has a power

$$P_u = P_0 \exp(-\sigma_\phi^2) G(\alpha) \quad , \quad (211)$$

where  $P_0$  is the power that would be received in the absence of scattering if the antenna has been pointed at the source.

If a parameter is defined relating the scattering to the antenna beamwidth,

$$u = 5.2 \cdot \overline{\psi^2} / \theta_b^2 \quad , \quad (212)$$

the radar components each have a voltage variance (i.e., mean power) given by

$$P_s = \frac{P_0}{2} [1 - \exp(-\sigma_\phi^2)] \frac{G(\alpha)}{\sqrt{u+1}} \exp\left[\frac{2.6\alpha^2}{\sigma_b^2} \frac{u}{1+u}\right]. \quad (213)$$

If the antenna is pointed at the source so that  $\alpha=0$ , the power can be considered to be an unmodified signal plus a randomly phased noise component. The "signal-to-noise" ratio in this representation is

$$S/N = \sqrt{u+1} \frac{e^{-\sigma_\phi^2}}{1 - e^{-\sigma_\phi^2}}. \quad (214)$$

It can be recognized that the amplitude distribution will be Rician.

### 5.8 Difference Channel Signal

The difference channel will also contain both an unmodified signal and a modified, scattered component. If the difference channel gain is  $\sin^2(p\alpha) G(\alpha/2)$ , which is normally zero for  $\alpha=0$ , the unmodified component (which is in quadrature to the unmodified sum channel component) has a power

$$P_{\Delta u} = P_0 \sin^2(p\alpha) G(\alpha/2) \exp(-\sigma_\phi^2). \quad (215)$$

The total power in the modified, random component will be

$$P_{\Delta s} = \frac{P_0}{\left(1 + \frac{u}{4}\right)^{3/2}} [1 - \exp(-\sigma_\phi^2)] G(\alpha'/2) \sin^2(p\alpha') \left[1 + \frac{\psi^2}{\alpha'^2}\right] \quad (216)$$

where  $\alpha' = \alpha/\sqrt{1+u/4}$  and  $p = 1.4/\sigma_b$ .

## 5.9 Limitations

The analysis has assumed that sufficient independent structures are encountered that the central limit theorem results in gaussian distributions of integrated phase and spatial derivative of phase, and the analysis has dropped terms that are significant only in the antenna near zone. Both these assumptions are valid for most problems of interest.

The angular power spectrum is not necessarily gaussian if  $\sigma_{\phi}^2 \ll 1$  but again this is not usually a regime of concern.

Possible correlations between the sum and difference channel signals have not been explored. Moreover, the specific analysis here assumed that the target displacement was along one axis of the monopulse difference beam and the striations were aligned with the other axis.

## REFERENCES

1. Chesnut, W., Private communication.
2. Kilb, R.W., "Striation Formation," High-Altitude Nuclear Weapons Effects, Defense Nuclear Agency (to be published).
3. Bogusch, R.L., W.F. Crevier, F.W. Guigliano, S.L. Gutsche, R.W. Hendrick, and R.W. Kilb, HARC: A Detailed Simulation of Radar Tracking Measurements in a High-Altitude Nuclear Environment, Mission Research Corporation, MRC-R-32 (U), July 1972.
4. Bramley, E.N., "The Diffraction of Waves by an Irregular Refracting Medium," Proc. Roy. Soc., Ser. A, Vol. 225, 1954, pp. 515-518.
5. Hendrick, R.W., On the Continuation of Gaussian Series, Mission Research Corporation, MRC-N-168, November 19, 1974.
6. Hendrick, R.W., W.A. Flood, and V.R. Stull of General Electric TEMPO, Wide Band Propagation in a Striated Environment, Mission Research Corporation, MRC-R-110 (U), January 1974.
7. Booker, H.G., J.A. Ratcliffe and D.H. Shinn, "Diffraction from an Irregular Screen with Applications to Ionospheric Problems," Trans. Roy. Soc., Ser. A, Vol. 242, 1950, pp. 579-607.
8. Ratcliffe, J.A., "Some Aspects of Diffraction Theory and Their Application to the Ionosphere," Reports on Progress in Physics, Vol. 19, The Physical Society, London, 1956.

APPENDIX A  
A USEFUL INTEGRAL

Consider an integral of the form

$$I = \int_{-\infty}^{\infty} P(x) \exp[-(ax^2 + bx + c)] dx \quad (A1)$$

where  $P(x)$  is a polynomial in  $x$  and  $a$ ,  $b$ , and  $c$  are complex constants (or functions of variables not involved in the integration). The processes needed to perform the integrations are straightforward but the arithmetic is often tedious.

The procedure is to use a linear transformation of variable to remove the linear term in the exponent. The constant term can then be taken outside the integration, leaving only the second power of the variable. The polynomial will have transformed into a new polynomial of the same order. The integral of odd order terms will be zero and the integral of even order terms is a well known definite integral. As an example, let the polynomial be a quadratic

$$P(x) = p_0 + p_1 x + p_2 x^2 \quad (A2)$$

Use the transformation

$$x = y - \frac{b}{2a} \quad (A3)$$

This produces

$$I = \int_{-\infty}^{\infty} \left[ \left( p_0 - \frac{bp_1}{2a} + \frac{b^2 p_2}{4a^2} \right) + \left( p_1 - \frac{bp_2}{a} \right) y + p_2 y^2 \right] \\ \times \exp \left( -a y^2 + \frac{b^2}{4a} - c \right) dy \quad (A4)$$

$$= \exp \left( \frac{b^2 - 4ac}{4a} \right) \int_{-\infty}^{\infty} \left( p_0 - \frac{bp_1}{2a} + \frac{b^2 p_2}{4a^2} + p_2 y^2 \right) \exp(-ay^2) dy \quad (A5)$$

This final integral has the value

$$I = \exp \left( \frac{b^2 - 4ac}{4a} \right) \sqrt{\frac{\pi}{a}} \left[ p_0 - \frac{bp_1}{2a} + \frac{b^2 p_2}{4a^2} + \frac{p_2}{2a} \right]. \quad (A6)$$

## DISTRIBUTION LIST

### DEPARTMENT OF DEFENSE

Assistant Secretary of Defense  
 Cmd, Cont, Comm, & Intell.  
 ATTN: J. Babcock  
 ATTN: M. Epstein

Director  
 Command Control Technical Center  
 ATTN: C-112, R. Mason  
 ATTN: C-650

Director  
 Defense Advanced Resch. Proj. Agency  
 ATTN: Nuclear Monitoring Research  
 ATTN: Strategic Tech. Office

Defense Communication Engineer Center  
 ATTN: Code R410, James W. Melan  
 ATTN: Code R820, R. L. Crawford

Director  
 Defense Communication Agency  
 ATTN: Code 810, R. W. Boulton  
 ATTN: Code 480  
 ATTN: Code 1010, Maj Reed  
 ATTN: Murray Ruffenberger

Defense Communication Agency  
 WWRCS System Engineer Lab Dept.  
 ATTN: R. L. Crawford

Defense Documentation Center  
 Cameron Station  
 Exec ATTN: TC

Director  
 Defense Intelligence Agency  
 ATTN: DT-10  
 ATTN: DC-70, W. White Jr

Director  
 Defense Nuclear Agency  
 ATTN: TISI, Archives  
 ATTN: DMST  
 Exec ATTN: TITL, Tech. Library  
 Exec ATTN: RAAE  
 ATTN: SCVI

Dir. of Defense Resch. & Engineering  
 ATTN: S888 (08)

Commander, Field Command  
 Defense Nuclear Agency  
 ATTN: FCPR

Director  
 Interagency Nuclear Weapons School  
 ATTN: Document Control

Director  
 Joint Strat. Tgt. Planning Staff, JCS  
 ATTN: JSTP, Capt G. D. Gooz  
 ATTN: JCTR-2

### DEPARTMENT OF DEFENSE (Continued)

Chief  
 Livermore Division, Field Command, DNA  
 Lawrence Livermore Laboratory  
 ATTN: FCPL

Director  
 National Security Agency  
 ATTN: Frank Leonard  
 ATTN: Pat Clark, W14  
 ATTN: John Skillingman, R52

OUCS/D-1  
 ATTN: WWCCE Eval. Ofc., Mr. Tom

### DEPARTMENT OF THE ARMY

Commander/Director  
 Atmospheric Sciences Laboratory  
 U.S. Army Electronics Command  
 ATTN: DRSEL-RL-D, R. Holt  
 ATTN: DRSEL-RL-SY-R, F. E. Niles

Director  
 BMD Advanced Tech. Ctr.  
 ATTN: ATC-T, Melvin T. Cappo  
 ATTN: ATC-O, W. Davies  
 ATTN: ATC-R, Don Ross

Program Manager  
 BMD Program Office  
 ATTN: BACS-BMF, John Shea

Chief of Services Division  
 U.S. Army Communication Cnd.  
 ATTN: CC-OPS-CC

Commander  
 Barry Blumond Laboratories  
 ATTN: DRXDO-TI, Mildred R. Weiner  
 ATTN: DRXDO-SP, Francis M. Minnetta  
 ATTN: DRXDO-EP, Cyrus Moagel

Director  
 TRASANA  
 ATTN: ATAA-TAC, LTC John Bense  
 ATTN: ATAA-SA  
 ATTN: TCC, F. Poyan, Jr.

Director  
 U.S. Army Ballistic Research Labs.  
 ATTN: Lawrence J. Pickett  
 ATTN: C. P. Keller, DRXDR-CA

Commander  
 U.S. Army Comm-Elec. Engrg. Instal. Argy  
 ATTN: EED-PEB, George Law

Commander  
 U.S. Army Electronics Command  
 ATTN: DRREL-RL-RD, R. S. Bennett

DEPARTMENT OF THE ARMY (Continued)

Commander  
U.S. Army Foreign Science & Tech. Ctr.  
ATTN: E. Jones  
ATTN: P. A. Crowley

Commander  
U.S. Army Materiel Dev. & Readiness Cnd.  
ATTN: BRCLDC, J. A. Aender

Commander  
U.S. Army Missile Command  
ATTN: BRSMI-XS, Chief Scientist  
ATTN: BRSMI-YTF, W. G. Proumell, Jr.  
ATTN: Chief, Doc. Section

Commander  
U.S. Army Missile Intelligence Agency  
ATTN: TMG Comdr

Commander  
U.S. Army Nuclear Agency  
ATTN: MORNA-3F, J. Barboret

Commander  
U.S. Army SALCOM Agency  
ATTN: Document Control

DEPARTMENT OF THE NAVY

Chief of Naval Operations  
ATTN: Alexander W. Wint  
ATTN: Ronald L. Puckley  
ATTN: LDR 001, OP 933

Chief of Naval Research  
ATTN: Code 48  
ATTN: Code 501

Commander  
Naval Electronic Systems Command  
Naval Electronic Systems C & Bgr.  
ATTN: PME 117-1, Satellite Comm. Proj. 001  
ATTN: PME 117  
ATTN: NAVALEV 011, T. Barry Hughes

Commanding Officer  
Naval Intelligence Support Ctr.  
ATTN: Mr. Daddino, STIC 12

Commander  
Naval Ocean Systems Center  
ATTN: Code 0100, C. Russell  
ATTN: Code 2700  
ATTN: William L. Meier

Director  
Naval Research Laboratory  
ATTN: Code 5300, Rg. Comm. Div., Bruce Kald  
ATTN: Code 5900, Electromag. Prop. Br.  
ATTN: Code 2700, Timothy P. Coffey  
ATTN: Code 2701, Jack D. Brown  
ATTN: Code 5604, Trans. Prop. Br.  
ATTN: Code 5700, Prop. Appl. Comm.  
ATTN: Code 2600, Tech. Lib.  
ATTN: Code 5300, Satellite Comm.  
ATTN: Code 2700, Edgar A. McClellan

DEPARTMENT OF THE NAVY (Continued)

Commander  
Naval Space Surveillance System  
ATTN: Capt. J. B. Burton

Officers-in-Charge  
Naval Surface Weapons Center  
ATTN: Code 6A501, Navy Nuc. Progm. Off.

Director  
Strategic Systems Project Office  
ATTN: NSP-2161  
ATTN: NSSP-2722, Fred Wimperly

DEPARTMENT OF THE AIR FORCE

Commander  
ADC/DC  
ATTN: DC, Mr. Long

Commander  
ADCOM/SPD  
ATTN: SP000

Atmospherics Laboratory, AFSC  
ATTN: PHD, John P. Mullen  
ATTN: OPR, Alva T. Stair  
ATTN: TKB, Kenneth S. W. Champlin  
ATTN: OPR, James C. Plwck  
ATTN: PHD, Jurgen Buchau  
ATTN: OPR, Harold Gardner  
ATTN: SCOL, Paul, Lib.  
ATTN: PHD, Jules Aarons

Air Weapons Laboratory, AFSC  
ATTN: SPL  
ATTN: CA, Arthur H. Gauthier  
ATTN: DYC, John M. Kamm  
ATTN: DYC, Capt. L. McIver

ADLAD  
ATTN: H/Maj Wiley  
ATTN: IN

Air Force Avionics Laboratory, AFSC  
ATTN: AAD, Wade Row  
ATTN: AAB, R. M. Hartman  
ATTN: AAB, Allen Johnson

Headquarters  
Electronic Systems Division/XR  
ATTN: XRC, Lt. Col. J. Martin  
ATTN: XRI, Lt. Michael

Headquarters  
Electronic Systems Division/YS  
ATTN: YSEY

Headquarters  
Electronic Systems Division, AFSC  
ATTN: Tim Deane

Commander  
Research Technicians Division, AFSC  
ATTN: TDB, B. L. Ballard  
ATTN: TDC, Library

DEPARTMENT OF THE AIR FORCE (Continued)

Sq. BSSE/RO  
ATTN: RDQ

Commander  
Rome Air Development Center, AFSC  
ATTN: V. Coyne, OCSE  
ATTN: FIELD, Doc. Library

Commander  
Rome Air Development Center, AFSC  
ATTN: ETL, A. Lorenzen

SAMSO/MN  
ATTN: MNX  
ATTN: MNRL, Lt Col Kennedy

SAMSO/SK  
ATTN: SKA, Lt Marie A. Clavin

SAMSO/SI  
ATTN: SSI, Maj Lawrence Bean

SAMSO/YA  
ATTN: YAF, Capt L. Blackwelder

Commander in Chief  
Strategic Air Command  
ATTN: SRI  
ATTN: ABRATE, Capt Bruce Bauer  
ATTN: SPIS, Maj Brian G. Stephan

ENERGY RESEARCH & DEVELOPMENT ADMINISTRATION

FERG, Inc.  
Los Alamos Division  
ATTN: James R. Breedlove  
ATTN: James L. Walker  
ATTN: J. D. M. Fu

University of California  
Lawrence Livermore Laboratory  
ATTN: Ralph S. Butler, 1-31  
ATTN: Terry P. Donnelly, 1-96  
ATTN: Donald R. Dunn, 1-156  
ATTN: Ronald L. Gill, 1-31  
ATTN: Tech. Inscr., Dept. 1-3

Los Alamos Scientific Laboratory  
ATTN: Doc. Com. for John Tom  
ATTN: Doc. Com. for Phil Jones  
ATTN: Doc. Com. for John S. Mott  
ATTN: Doc. Com. for R. L. French

Sandia Laboratories  
ATTN: Doc. Com. for W. D. Brown, Org. 1101  
ATTN: Doc. Com. for L. Wright  
ATTN: Doc. Com. for S. C. Edwards, Org. 1200  
ATTN: Doc. Com. for S. A. Pahlstrom, Org. 1227  
ATTN: Doc. Com. for Clarence R. Mohl, Org. 1300  
ATTN: Doc. Com. for A. Dean Giesler, Org. 1375  
ATTN: Doc. Com. for Al. Sandt, Rpt. 1011  
ATTN: Doc. Com. for Charles Williams  
ATTN: Doc. Com. for L. P. Martin, Org. 1300

OTHER GOVERNMENT AGENCIES

Department of Commerce  
Office of Telecommunications  
Institute for Telecom Science  
ATTN: William F. Blunt  
ATTN: L. A. Berry  
ATTN: G. Reed

NASA  
Goddard Space Flight Center  
ATTN: ATS-6 Ocr., P. Corrigan

National Oceanic & Atmospheric Admin.  
Environmental Research Laboratory  
ATTN: RY, Donald J. Williams  
ATTN: Richard Grubb  
ATTN: C. L. Rufenach  
ATTN: Joseph D. Pope

DEPARTMENT OF DEFENSE CONTRACTORS

Aerospac Corporation  
ATTN: F. A. Morse, Ab, Rm. 2507  
ATTN: F. E. Bond, Ab, Rm. 5003  
ATTN: Irving M. Garfunkel  
ATTN: S. P. Bowser  
ATTN: J. E. Carter, 120, Rm. 2209  
ATTN: G. W. Anderson  
ATTN: Walter Grabowky  
ATTN: Norman D. Stockwell  
ATTN: V. Josephson  
ATTN: T. M. Sidel  
ATTN: B. F. Olson, 120, Rm. 2206E

Aeronomy Corporation  
ATTN: S. A. Roschell

Analytical Systems Engineering Corp.  
ATTN: Radio Sciences

De Boeing Company  
ATTN: Glen Seifert  
ATTN: D. Murray

Brown Engineering Company, Inc.  
Cambridge Research Lab.  
ATTN: Romeo A. DeLiberis  
ATTN: S. Pasolun

California State University at San Diego  
Radio Physics Lab. at the Scripps  
Institute of Oceanography  
ATTN: Peter C. Bostet

Charles Stark Draper Laboratory, Inc.  
ATTN: D. M. Cox  
ATTN: S. P. Chimento, 98-61

Computer Sciences Corporation  
ATTN: R. Blank

COMET Electronics  
ATTN: R. R. Galt

Cornell University  
Department of Electrical Engineering  
ATTN: D. L. Taylor, Jr.

## DEPARTMENT OF DEFENSE CONTRACTORS (Continued)

## BSL, Inc.

ATTN: J. Roberts  
 ATTN: James Marshall  
 ATTN: V. L. Mower  
 ATTN: C. W. Prettie

## Ford Aerospace &amp; Communications Corp.

ATTN: J. T. Hattlingloy, MS X22

General Electric Company  
 Space Division  
 Valley Forge Space Center

ATTN: M. H. Berner, Space Sci. Lab.  
 ATTN: Robert H. Edsall

General Electric Company  
 TEMPO-Center for Advanced Studies

ATTN: Don Chandler  
 ATTN: Mack Stanton  
 ATTN: Warren S. Knapp  
 ATTN: Tom Barrett  
 ATTN: Tim Stephens  
 ATTN: William F. Namera  
 ATTN: B. Cambell  
 ATTN: DAFIAC

## General Electric Company

ATTN: George P. Millman  
 ATTN: F. A. Reibert

## General Research Corporation

ATTN: John Lee, Jr.  
 ATTN: Joel Garbarino

## Geophysical Institute

University of Alaska  
 ATTN: Technical Library  
 ATTN: T. N. Davis  
 ATTN: Neal Wilson

## GTE Sylvania, Inc.

ATTN: Marshall Crook

## Harris Corporation

Harris Semiconductor Division  
 ATTN: Carl E. Davis, MS 178-270

## HSS, Inc.

ATTN: Donald Hansen

## University of Illinois

Department of Electrical Engineering  
 ATTN: R. C. Yeh

## Institute for Defense Analyses

ATTN: Ernest Bauer  
 ATTN: Joel Bengtson  
 ATTN: Hans Woldhard  
 ATTN: J. M. Actin

## Int'l. Tel. &amp; Telegraph Corporation

ATTN: Technical Library

## IRT Corporation

ATTN: F. De Plamp

## Linceo

ATTN: S. R. Goldman

## DEPARTMENT OF DEFENSE CONTRACTORS (Continued)

## Johns Hopkins University

Applied Physics Laboratory  
 ATTN: Document Librarian  
 ATTN: Thomas Potempa  
 ATTN: John Dascalos

## Kaman Sciences Corporation

ATTN: F. G. Foxwell

## Linkabit Corporation

ATTN: Irwin Jacobs

## Lockheed Martin &amp; Space Co., Inc.

ATTN: D. R. Churchill  
 ATTN: Dept. 60-12

## Lockheed Martin &amp; Space Co., Inc.

ATTN: Martin Kull, Dept. 52-10  
 ATTN: Robert H. An  
 ATTN: Richard C. Johnson, Dept. 52-12

## MIT Lincoln Laboratory

ATTN: Mr. Malden, X111  
 ATTN: David M. Towle, L10, A-082  
 ATTN: D. Clark  
 ATTN: James R. Pannell, L-246  
 ATTN: J. V. Evans

## Martin Marietta Aerospace

Orlando Division  
 ATTN: Roy W. Jettner

## Martin Marietta Corporation

Denver Division  
 ATTN: B. J. Bittner

## McDonnell Douglas Corporation

ATTN: George Price  
 ATTN: William Olson  
 ATTN: Robert W. Halprin  
 ATTN: J. Mauls  
 ATTN: S. Barfo

## Hawthorn Research Corporation

ATTN: R. Bendicef  
 ATTN: M. Scheide  
 ATTN: Ralph Ellb  
 ATTN: D. Sappenfield  
 ATTN: Dave Bowle  
 ATTN: F. Eiden  
 ATTN: W. P. Croyler  
 ATTN: Steven L. Gutache  
 ATTN: Warren A. Schlueter  
 ATTN: R. Rogusch  
 ATTN: L. Shaeffer  
 ATTN: Tech. Library

## The MITRE Corporation

ATTN: Chief Scientist, W. Soc.  
 ATTN: J. C. Kennan  
 ATTN: C. F. Callahan  
 ATTN: G. Harding

## Pacific-Sterra Research Corp.

ATTN: F. C. Field, Jr.

## Photometrics, Inc.

ATTN: Irving L. Rotaky

DEPARTMENT OF DEFENSE CONTRACTORS (Cont Inued)

Physical Dynamics, Inc.

ATTN: E. J. Fremouw

Physical Dynamics, Inc.

ATTN: Joseph B. Workman  
ATTN: A. Thompson

The Trustees of Princeton University  
Forrestal Campus Library

ATTN: F. W. Perkins, Plasma Physics Lab.

R&D Associates

ATTN: R. P. Turco  
ATTN: H. A. Ory  
ATTN: Forrest Gilmore  
ATTN: William B. Wright, Jr.  
ATTN: Bryan Galsbard  
ATTN: Robert E. Leveyet  
ATTN: William J. Karzas

The Rand Corporation

ATTN: Ed Bedrosian  
ATTN: Colleen Crain

Raytheon Company

ATTN: C. D. Thome  
ATTN: Barbara Adams

Riverside Research Institute

ATTN: R. Popelow

Science Applications, Inc.

ATTN: Jack McDaniel  
ATTN: Raymond C. Lee  
ATTN: Curtis A. Smith  
ATTN: Daniel A. Hamlin  
ATTN: D. Sachs

Science Applications, Inc.  
Burlington Division

ATTN: Dale H. Davis

DEPARTMENT OF DEFENSE CONTRACTORS (Cont Inued)

SRI International

ATTN: Robert S. Leonard  
ATTN: G. Smith  
ATTN: Walter G. Chosma  
ATTN: J. G. Depp  
ATTN: Walter Jaye  
ATTN: Ray L. Leadabrand  
ATTN: M. Baron  
ATTN: Charles L. Rino

System Development Corporation

ATTN: E. G. Meyer

Tri-Com, Inc.

ATTN: Darrel Murray

TRW Defense & Space Sys. Group

ATTN: Robert M. Webb, RI-2310  
ATTN: R. K. Piebach, RI-2078

VisIDyne, Inc.

ATTN: J. W. Carpenter  
ATTN: Charles Humphrey